DMD Fast Forward. Published on November 5, 2007 as DOI: 10.1124/dmd.107.018416
DMD Fast Forward. Published on November 5, 2007 as doi:10.1124/dmd.107.018416
This article has not been copyedited and formatted. The final version may differ from this version.

DMD #18416

Reductive Isoxazole Ring-Opening of the Anticoagulant Razaxaban Is the Major Metabolic Clearance Pathway in Rats and Dogs

Donglu Zhang, Nirmala Raghavan, Shiang-Yuan Chen, Haiying Zhang, Mimi Quan, Lloyd Lecureux, Laura M. Patrone, Patrick Y.S. Lam, Samuel J. Bonacorsi, Robert M. Knabb, Gary L. Skiles, and Kan He

Pharmaceutical Candidate Optimization (DZ, NR, HZ, LL, GLS, KH), Drug Safety Evaluation (LMP), Discovery Chemistry (MQ, PYSL), Radiochemistry (SC, SJB), and Discovery Biology (RMK), Bristol-Myers Squibb Research and Development, Princeton, NJ 08543

Downloaded from dmd.aspetjournals.org at ASPET Journals on April 17, 2024

Copyright 2007 by the American Society for Pharmacology and Experimental Therapeutics.

DMD Fast Forward. Published on November 5, 2007 as DOI: 10.1124/dmd.107.018416
This article has not been copyedited and formatted. The final version may differ from this version.

Running title: Reductive Isoxazole Ring-opening of Razaxaban

Address correspondence to:

Donglu Zhang, Ph.D.

Pharmaceutical Candidate Optimization,

Bristol-Myers Squibb Research and Development, P.O. BOX 4000,

Princeton, NJ 08543, Phone: 609-252-5582.

Email: Donglu.Zhang@BMS.com

[1]Abbreviations used: BDC, bile-duct cannulation; CYP, cytochrome P450; HPLC, high performance liquid chromatography; HLM, human liver microsomes; LC/MS, liquid chromatography/mass spectrometry; NMR, nuclear magnetic resonance; NADH, β-nicotinamide adenine dinucleotide sodium (reduced form); NADPH, β-nicotinamide adenine dinucleotide phosphate sodium (reduced form); TFA, trifluoroacetic acid; TLC, thin layer chromatography

Text pages including references: 31

# of tables: 4; # of figures: 9

# of references: 27

# of words in abstract: 245

# of words in introduction: 500

# of words in discussion: 1000

Downloaded from dmd.aspetjournals.org at ASPET Journals on April 17, 2024

DMD Fast Forward. Published on November 5, 2007 as DOI: 10.1124/dmd.107.018416
This article has not been copyedited and formatted. The final version may differ from this version.

Abstract

Razaxaban is a selective, potent, and orally bioavailable inhibitor of coagulation factor Xa. The molecule contains a 1,2-benzisoxazole structure. Following oral administration of [^{14}C]razaxaban to intact and bile duct-cannulated rats (300 mg/kg) and dogs (20 mg/kg), metabolism followed by biliary excretion was the major elimination pathway in both species, accounting for 34-44% of the dose, while urinary excretion accounted for 3-13% of the dose. Chromatographic separation of radioactivity in urine, bile, and feces of rats and dogs showed that razaxaban was extensively metabolized in both species. Metabolites were identified based upon LC/MS/MS and comparison with synthetic standards. Among the twelve metabolites identified, formation of an isoxazole-ring opened benzamidine metabolite (M1) represented a major metabolic pathway of razaxaban in rats and dogs. However, razaxaban was the major circulating drug-related component (>70%) in both species and M1, M4, and M7 were minor circulating components. In addition to the *in vivo* observations, M1 was formed as the primary metabolite in rat and dog hepatocytes, and in rat liver cytosolic fraction. The formation of M1 in the rat liver fraction required the presence of NADH. Theses results suggest that isoxazole ring reduction, forming a stable benzamidine metabolite (M1), represents the primary metabolic pathway of razaxaban *in vivo* and *in vitro*. The reduction reaction was catalyzed by NADH-dependent reductase(s) in the liver and possibly by intestinal microflora based on the recovery of M1 in feces of bile duct-cannulated rats.

Downloaded from dmd.aspetjournals.org at ASPET Journals on April 17, 2024

DMD Fast Forward. Published on November 5, 2007 as DOI: 10.1124/dmd.107.018416
This article has not been copyedited and formatted. The final version may differ from this version.

Introduction

Thromboembolic disorders, including acute myocardial infarction, deep vein thrombosis, pulmonary embolism, and ischemic stroke, continue to be the leading cause of morbidity and mortality in the US and other Western countries. Current therapies for the treatment and prevention of thrombotic disorders are inadequate because they require parenteral administration of heparins or careful monitoring of clotting times during warfarin therapy to achieve desired efficacy and minimize excessive bleeding (Stein et al., 1994). Therefore, there is a significant medical need for safer and more effective orally active anticoagulants.

Factor Xa is a key serine protease in the coagulation cascade and has been shown to be a promising target enzyme for the treatment and prevention of arterial and venous thrombosis (Walenga et al., 2003; Samama 2002). Extensive preclinical and clinical studies show that inhibition of factor Xa is effective in both venous and arterial thrombosis (Walenga et al., 2003). In animal models a better therapeutic index (antithrombotic efficacy vs antihemostatic effects) has been shown for direct factor Xa inhibitors compared to direct thrombin inhibitors (Wong et al., 2007; Wong et al., 2002 a and b; Leadley 2001).

Razaxaban (BMS-561389, DPC906), 1-(3'-aminobenzisoxazol-5'-yl)-3-trifluoromethyl-N-[2-fluoro-4-(2'-dimethyl aminomethylimidazol-1-yl)phenyl]-1H-pyrazole-5-carboxy-amide, is a highly potent and selective factor Xa inhibitor. Razaxaban showed potent antithromobotic efficacy in animal models and in patients with deep vein thrombosis

Downloaded from dmd.aspetjournals.org at ASPET Journals on April 17, 2024

DMD Fast Forward. Published on November 5, 2007 as DOI: 10.1124/dmd.107.018416
This article has not been copyedited and formatted. The final version may differ from this version.

(Wong et al., 2007). The chemical structure of razaxaban contains an isoxazole ring (Figure 1).

The 1,2-isoxazole substructure of several drugs and drug candidates has been reported to undergo extensive reductive isoxazole ring opening leading to imine intermediates that hydrolyze to ketone-containing products (Stiff et al., 1992; Mannens et al., 1993; Mutlib et al., 1995; Yuan et al., 2003). The facile reductive cleavage of the N-O bond have been attributed to the greater electronegativity of the nitrogen atom adjacent to the oxygen in the isoxazole ring (Dalvie et al., 2002; Kalgutkar et al., 2003; Tschirret-Guth and Wood 2003), a feature that is absent in the oxazole ring system that exclusively undergoes oxidative ring opening (Dalvie et al., 2003; Li et al., 2006). In this study, we report the reductive 1,2-benzisoxazole ring opening of razaxaban to form a stable benzamidine metabolite.

Downloaded from dmd.aspetjournals.org at ASPET Journals on April 17, 2024

DMD Fast Forward. Published on November 5, 2007 as DOI: 10.1124/dmd.107.018416
This article has not been copyedited and formatted. The final version may differ from this version.

Materials and Methods

Materials and general equipment

Razaxaban and the advanced intermediate (BMS-564372) were synthesized at Bristol-Myers Squibb Company. Potassium [^{14}C]cyanide (52.5 mCi/mmol) was purchased from PerkinElmer Life Sciences (Boston, MA). The chemical structure and the position of the C-14 label of [^{14}C]razaxaban are shown in Figure 1. The specific activity of [^{14}C]razaxaban was 34.67 μCi/mg (98.8% of radioactivity purity and 99% of chemical purity). Ammonium bicarbonate was purchased from Fischer Scientific Co. (Fair Lawn, NJ). Alcohol dehydrogenase from equine livers (0.5 units/mg) and aldehyde dehydrogenase from yeast (20 unit/mg) were purchased from Sigma Aldrich (St. Louis, MO). Ecolite™ liquid scintillation cocktail was purchased from ICN Biomedicals, Inc. (Costa Mesa, CA). Cryopreserved hepatocytes from male beagle dogs were purchased from In Vitro Technologies (Baltimore, MD). Fresh hepatocytes from male Sprague-Dawley rats were prepared in house using a literature method (Berry and Friend, 1969). All other organic solvents and the reagents were of HPLC grade and reagent grade.

Deepwell LumaPlate™96-well plates were purchased from PerkinElmer Life Sciences (Boston, MA); automatic Environmental Speed Vac was obtained Savant (Holbrook, NY); Eppendorf 5810 R centrifuge was acquired Eppendorf Company (Hamburg, Germany); Packard Microplate Scintillation and Luminescence Counter (models Top Count NXT) was purchased PerkinElmer Life Sciences (Meriden, CT); a fraction collector was from Gilson Medical Electronics (Middleton, WI); NMR Spectra were recorded on a 300 MHz Bruker Biospin spectrometer (Bruker, Boston).

Downloaded from dmd.aspetjournals.org at ASPET Journals on April 17, 2024

DMD Fast Forward. Published on November 5, 2007 as DOI: 10.1124/dmd.107.018416
This article has not been copyedited and formatted. The final version may differ from this version.

Synthesis of [^{14}C]razaxaban

Radiolabeled [^{14}C]razaxaban was prepared as illustrated in Figure 2. [^{14}C]KCN was used to prepare Zn(^{14}CN)$_2$ which was reacted with an advanced aryl bromide to provide the labeled penultimate intermediate. The final product (radiochemical yield 43%) was isolated as its HCl salt following HPLC purification. The radiochemical purity of [^{14}C]razaxaban was 98.8%, and its specific activity was 34.67 μCi/mg.

3-Bromo-4-fluoronitrobenzene (**1**). Potassium bromate (18.7 g, 112 mmol) was added in portions to a suspension of 4-fluoronitrobenzene (14.1 g, 100 mmol) in a mixture of H_2SO_4 (7 mL) and water (7 mL) at 80°C with stirring. After 3 h, the mixture was poured onto ice. The precipitate was collected by filtration, dissolved in dichloromethane (100 mL), dried over Na_2SO_4, filtered, and evaporated to dryness to give the intermediate **1** (14 g, 64.5%). ^{1}H NMR ($CDCl_3$) δ 8.60 (1H, dd), 8.32 (1H, m), 7.90 (1H, t).

3-Bromo-4-fluoroaniline (**2**). To a solution of **1** (11.0 g, 50 mmol) in acetic acid (100 mL), iron powder (5.5 g, 98 mmol) was added in small portions. The mixture was stirred at room temperature for 2 h then poured onto ice (200 g). The oily product was dissolved in dichloromethane and purified by column chromatography eluted with hexane / dichloromethane (1:1, v/v) to give the intermediate **2** (15 g, 80%). ^{1}H NMR ($CDCl_3$) δ 6.88 (1H , s), 6.83 (1H, m), 6.53 (1H, m).

1-(4'-Fluoro-3'-bromophenyl)-3-trifluoromethyl-5-furyl-1H-pyrole (**3**). To **2** (8 g, 42 mmol) in concentrated HCl (80 mL) at -5°C was added drop-wise, a solution of sodium nitrite (5.8 g, 82 mmol) in water (10 mL) maintaining the temperature < 4°C. The reaction mixture was stirred at 0°C for 30 min. Stannous chloride dihydrate (29.7 g, 126 mmol) dissolved in concentrated HCl (20 mL) at 0°C was added drop-wise to the reaction

Downloaded from dmd.aspetjournals.org at ASPET Journals on April 17, 2024

DMD Fast Forward. Published on November 5, 2007 as DOI: 10.1124/dmd.107.018416
This article has not been copyedited and formatted. The final version may differ from this version.

mixture with stirring. After 30 min a solution of 4,4,4-trifluoro-1-(2-furyl)-2,4-butanedione (8.65 g, 42 mmol) dissolved in acetic acid (50 mL) and methanol (100 mL) was added, and stirring was continued for 16 h at room temperature. The reaction mixture was diluted with water (100 mL) and extracted with dichloromethane (100 mL x2). After solvent removal, the residue was purified by column chromatography eluted with hexane/ethyl acetate (4:1, v/v) giving the intermediate **3** (4 g, 10.7 mmol, 25%). ^{1}H NMR ($CDCl_3$) δ 7.7 (1H, dd), 7.42 (1H, d), 7.35(1H, m), 7.2 (1H, t), 6.88 (1H, s), 6.4 (1H, m), 6.16 (1H, d). MS m/z 376 $[M+H]^+$.

1-(4'-Fluoro-3'-bromo-phenyl)-3-trifluoromethyl-1H-pyrole-5-carboxylic acid (**4**). To a mixture of **3** (11.25 g, 30 mmol) in acetonitrile (20 mL), $NaH_2PO_4.H_2O$ (20 g, 145 mmol) in water (20 mL) and phosphoric acid (1.2 mL) at -5°C was added sodium chlorite (31 g, 342 mmol) in water (60 mL) drop-wise maintaining the temperature under 0°C. The mixture was then stirred at ambient temperature for 4 h, then acidified with concentrated HCl (3.3 mL) and extracted with t-butyl methyl ether (84 mL). After solvent removal, the residue was purified by flash chromatography eluted with dichloromethane /methanol /acetic acid (20:2:1, v/v/v) giving **4** (8 g, 22.6 mmol, 75%). ^{1}H NMR ($CDCl_3$) δ 7.7 (1H, dd), 7.4 (1H, m), 7.36 (1H, s), 7.22 (1H, d). MS m/z 352 $[M+H]^+$.

1-(3'-Bromo-4'-fluorophenyl)-3-trifluoromethyl-N-[2-fluoro-4-[(2'-pyrrolidin-1-ylmethyl)-imidazol-1-yl]phenyl]-1H-pyrazole-5-carboxyamide (**5**). To a suspension of **4** (3.53 g, 10 mmol) in dichloromethane (30 mL) was added oxalyl chloride (2 M in dichloromethane, 10 mL) and DMF (0.1 mL). The mixture was stirred at room temperature for 30 min, then heated at 40°C for 1 h. The mixture was evaporated to dryness. The residue was dissolved in dichloromethane (30 mL), and added drop-wise to

Downloaded from dmd.aspetjournals.org at ASPET Journals on April 17, 2024

DMD Fast Forward. Published on November 5, 2007 as DOI: 10.1124/dmd.107.018416
This article has not been copyedited and formatted. The final version may differ from this version.

a solution of dimethylaminopyridine (1.2 g, 9.8 mmol) and BMS-564372 (2.4 g, 10 mmol) in dichloromethane (30 mL) at 0°C. The mixture was stirred at ambient temperature for 16 h. The solution was washed with water (10 mL), dried (Na_2SO_4), filtered, and concentrated. Flash column chromatography eluted with 5% methanol in dichloromethane on Celite® produced **5** (4.3 g 7.5 mmol, 75%) as a white solid. ^{1}H NMR ($CDCl_3$) δ 8.31 (1H, t), 8.10 (1H, s), 7.79 (1H, dd), 7.68 (1H, dd), 7.48 (1H, m), 7.36 (1H, d), 7.22 (1H, t), 7.17 (1H, s), 7.08 (2H, s), 3.40 (2H, s), 2.30 (6H, s). MS m/z 569 and 571 $[M+H]^+$.

1-[3'-Cyano(^{14}C)-4'-fluorophenyl]-3-trifluoromethyl-N-[2-fluoro-4-(2'-dimethylaminomethyl)imidazol-1-yl]phenyl-1H-pyrarole-5-carboxyamide (**6**). To $K^{14}CN$ (100 mCi, 1.90 mmol) in 0.5 mL water was added zinc chloride (116 mg, 0.853 mmol) in water (1 mL). The mixture was stirred for 10 min at room temperature. The mixture was lyophilized under high vacuum, and dried to constant weight at 75°C for 3 h. [^{14}C]Zinc cyanide was used directly for the subsequent cyanation. A round-bottomed flask was added with **5** (968 mg, 1.7 mmol), [^{14}C]zinc cyanide (100 mCi), and $pd_2(dba)_3$ (tris(dibenzylideneacetone) dipalladium) (85 mg), zinc powder (43 mg), dppf (1,1'-bis(diphenylphosphine)ferrocene, 85 mg) and DMF (40 mL) under nitrogen. The mixture was heated at 120°C for 4 h, cooled to room temperature, and diluted with ethyl acetate (200 mL) and washed with water (3 x 50 mL). The ethyl acetate solution was separated, dried over Na_2SO_4, filtered and evaporated to dryness. The residue was dissolved in dichloromethane. Flash chromatography eluted with 3% methanol in dichloromethane on Celite® produced 765 mg (78 mCi, 1.48 mmol, 78%) of **6** (radiochemical purity 97%). ^{1}H

Downloaded from dmd.aspetjournals.org at ASPET Journals on April 17, 2024

DMD Fast Forward. Published on November 5, 2007 as DOI: 10.1124/dmd.107.018416
This article has not been copyedited and formatted. The final version may differ from this version.

NMR ($CDCl_3$) δ 8.3 (1H, t), 8.2 (1H, b), 7.8 (2H, m), 7.7 (1H, dd), 7.38 (2H, m), 7.2 (1H, s), 3.4 (2H, s), 2.3 (6H, s).

1-(3'-Amino-3'-^{14}C-benzisoxazol-5-yl)-3-trifluoromethyl-N-[2-fluoro-4-(2'-dimethylaminomethyl)imidazol-1-yl]phenyl-1H-pyrazole-5-carboxylamide (**7**). To a mixture of **6** (295 mg, 0.57 mmol, 30 mCi), acetohydroxamic acid (128 mg) and potassium carbonate (475 mg) was added DMF (3.6 mL) and water (0.5 mL). The mixture was stirred at room temperature for 4 h. The mixture was diluted with ethyl acetate (50 mL), washed with water (10 mL x2), then evaporated to dryness. The residue was dissolved in methanol (20 mL) and purified by HPLC on a Zorbax C18, 21.2 x 250 mm column with a linear gradient of 0 min 20%B, 15 min 60%B, 20 min 95%B, 25 min 95%B, and 30 min 20%B and two solvents of A = water with 0.05% TFA and B = acetonitrile with 0.05% TFA. The product containing fractions were collected, combined, and freeze-dried. The residue was dissolved in ethyl acetate (20 mL), washed with 1N KOH (5 mL x2), water (5 mLx2), dried with Na_2SO_4, filtered and evaporated to dryness. The product (177 mg, 16.8 mCi, 56%) was dissolved in ethyl alcohol (20 mL). To this solution was added 1N HCl (0.32 mL). The solution was evaporated to dryness to yield BMS-561389 (303 mg). Specific activity was determined gravimetrically to be 34.67 μCi/mg. The radiochemical purity was 98.8% as determined by HPLC. NMR confirms this radioactive material to the structure of BMS-561389.

Synthesis of metabolite standards

M1. *N*-[4-(2-Dimethylaminomethyl)-1*H*-imidazol-1-yl-2-fluorophenyl]-1-(3-amidino-4-hydroxyphenyl)-3-trifluoromethyl-1*H*-pyrazole-5-carboxamide. Razaxaban (57 mg) was hydrogenated with 10% Pd/C (5 mg) and methanol (20 mL) at 35 psi for 30 min. The

Downloaded from dmd.aspetjournals.org at ASPET Journals on April 17, 2024

DMD Fast Forward. Published on November 5, 2007 as DOI: 10.1124/dmd.107.018416
This article has not been copyedited and formatted. The final version may differ from this version.

mixture was filtered through Celite®, concentrated, and dried to give 33.5 mg of the desired product. ^{1}H NMR (MeOH-d_4) δ 7.94 (t, 1H), 7.81 (d, 1H), 7.64 (dd, 1H), 7.40 (d, 1H) 7.34 (d, 3H), 7.06 (s, 1H), 6.75 (d, 1H), 3.45 (s, 2H), 2.20 (s, 6H). MS m/z 531.1 $[M+H]^+$.

M4. *N*-[4-(2-Methylaminomethyl-1*H*-imidazol-1-yl)-2-fluorophenyl]-1-(3-amino-1,2-benzisoxazol-5-yl)-3-trifluoromethyl-1*H*-pyrazole-5-carboxamide, bis(trifluoroacetic acid) salt. M4 was synthesized as described previously (Guan et al., 2005).

M5. *N*-[4-(2-Methylaminomethyl-1*H*-imidazol-1-yl)-2-fluorophenyl]-1-(3-amidino-4-hydroxyphenyl)-3-trifluoromethyl-1*H*-pyrazole-5-carboxamide, bis(trifluoroacetic acid) salt. Metabolite M4 (100 mg) was hydrogenated with 10% Pd/C (10 mg) and methanol (20 mL) at 35 psi for 30 min. The mixture was filtered through Celite®, concentrated, and dried to give 58 mg of the desired product as the bisTFA salt. ^{1}H NMR (MeOH-d_4) δ 7.93 (t, 1H), 7.81 (d, 1H), 7.64 (dd, 1H), 7.40 (m, 3H) 7.30 (d, 1H), 7.28 (s, 1H), 7.12 (d, 1H), 4.29 (s, 2H), 2.74 (s, 3H), 2.01 (s, 2H). MS (ESI) m/z 517.3 $[M+H]^+$.

M7. *N*-[4-(2-Hydroxymethyl-1*H*-imidazol-1-yl)-2-fluorophenyl]-1-(3-amino-1,2-benzisoxazol-5-yl)-3-trifluoromethyl-1*H*-pyrazole-5-carboxamide, trifluoroacetic acid salt. M7 was synthesized as described previously (Guan et al., 2005).

M10. To a solution of razaxaban (5.06 g) in chloroform (40 mL) and methanol (120 mL) was added 35% H_2O_2 (20 mL) at room temperature. The reaction mixture was stirred at room temperature over 66 h. Water (180 mL) was then added to the reaction mixture and the resulting slurry was stirred for 30 min. The solid was collected by filtration and dried in *Vacuo* with nitrogen purge at room temperature to a constant weight (3.97 g).

Downloaded from dmd.aspetjournals.org at ASPET Journals on April 17, 2024

DMD Fast Forward. Published on November 5, 2007 as DOI: 10.1124/dmd.107.018416
This article has not been copyedited and formatted. The final version may differ from this version.

Animal studies

[^{14}C]Razaxaban dose suspension was prepared in 0.5% aqueous methylcellulose at 25 mg/mL as a free base and administered to rats and dogs by oral gavage. Mid-toxicological doses at 300 mg/kg for rats and 30 mg/kg for dogs were used in the metabolism studies.

Sprague-Dawley rats (approximately 250 g) were fasted for approximately 11 h prior to dose administration. [^{14}C]Razaxaban was administered at 300 mg/kg (100 μCi/kg, and 12 mL/kg) as a single oral dose by gavage. Each dosing syringe was weighed immediately prior to and after dosing, and the exact quantity of formulation administered was determined gravimetrically from the difference. The rats were euthanized by carbon dioxide asphyxiation over dry ice, which was performed in accordance with American Veterinary Medical Association (AVMA) guidelines. Blood was collected by cardiac puncture under CO_2 anesthesia into tubes containing potassium EDTA at 1, 6, 12, and 24 h post-dose from 3 rats per time point. The tubes of whole blood were placed on ice before plasma was prepared by centrifugation within 30 min of sample collection. Livers were also collected from these rats after blood collection. The livers were flash frozen in liquid nitrogen and stored at −70±10°C. For BDC rats, intraduodenal infusion of a bile salt replacement solution was at approximately 1 mL/h. The bile salt replacement solution was prepared by adding approximately 18.0 g of cholic acid per 1 L of 0.9% sodium chloride solution followed by addition of sodium bicarbonate (approximately 1.3 g) to pH 7.4 (adjusted with hydrochloric acid), and sterile-filtering through 0.2 μm filters into sterile Viaflex bags. Bile was collected at 0-6, 6-24, and 24-48 h post dose into reservoirs that were surrounded by solid carbon dioxide. Urine was collected at 24-h

Downloaded from dmd.aspetjournals.org at ASPET Journals on April 17, 2024

DMD Fast Forward. Published on November 5, 2007 as DOI: 10.1124/dmd.107.018416
This article has not been copyedited and formatted. The final version may differ from this version.

intervals through 48 h post-dose. The samples were collected into containers surrounded by solid carbon dioxide. Feces were collected at ambient temperature at 24-h intervals through 48 h post dose.

Beagle dogs were fasted for approximately 14.5 h prior to single oral dose administration (20 mg/kg, 30 μCi/kg, 0.8 mL/kg) in a similar dosing procedure to rats by gavage. Blood samples were collected from 2 dogs (10 mL per time point) into tubes containing potassium EDTA at 1, 6, 12, and 24 h post dose. Samples were collected from the left or right jugular vein within ±5% of the scheduled time (≤ 24 h) or within 72 min of the scheduled time (> 24 h). The blood samples were placed on ice before plasma was prepared by centrifugation within 30 min of blood collection. The bile salt replacement solution that was used for the BDC rats was administered to BDC dogs via the distal (flushing) catheter at a rate of approximately 23 mL/kg/day. The balloon within the bile duct cannula was inflated to the appropriate volume and a right-angle Huber needle was inserted into the access port connected to the collection catheter. Bile was collected from 2 dogs at 0-6, 6-24, and 24-48 h post dose into reservoirs that were surrounded by solid carbon dioxide. Following the final bile collection, the balloon within the bile duct cannula was deflated and the normal bile flow pattern was re-established. Urine was collected at 24-h intervals through 48 h post dose into containers surrounded by solid carbon dioxide. Feces were collected at ambient temperature at 24-h intervals through 48 h post dose.

Water was added to each fecal sample (20%, w/w) before homogenization using a probe-type homogenizer.

Downloaded from dmd.aspetjournals.org at ASPET Journals on April 17, 2024

DMD Fast Forward. Published on November 5, 2007 as DOI: 10.1124/dmd.107.018416
This article has not been copyedited and formatted. The final version may differ from this version.

HPLC analysis

Sample analysis by high performance liquid chromatography (HPLC) was performed on a Shimadzu LC-10AT system equipped with a photodiode array ultraviolet (UV) detector from Shimadzu Scientific Instruments (Kyoto, Japan). A Xterra MS C18, 3.5 μ, 4.6 x 150 mm column (Waters, Corporation, Milford, MA) was used. The mobile phase flow rate was 1 mL/min. The retention times of reference standards were confirmed by the UV detection. The HPLC solvent system was a gradient and consisted of two solvents: A) 100% of 0.01 M ammonium bicarbonate, pH 9.0 and B) 100% acetonitrile. The step-linear gradient for elution was from 5 to 20% B in 5 min, from 20 to 40% B in 50 min, and then from 40 to 80% B in 5 min followed by hold at 80% B for 3 min before return to 5% B.

Preparation of biological samples for analysis

A 1 mL-portion of dog or rat urine or bile sample was loaded onto an Oasis (Waters) 3 mL solid phase cartridge which was conditioned by 1 column of methanol and 3 columns of water. The sample was allowed to go through the column under gravity and then eluted with 1 mL of acetonitrile. The eluent was evaporated under nitrogen, reconstituted with 200 μL of acetonitrile/water mixture (50:50, v/v), and vortexed. Following centrifugation at 2000xg for 5 min, a 20-μL portion was injected for HPLC analysis.

Each pooled plasma sample was extracted by addition of 5 mL of methanol and 1 mL of acetonitrile to 1 mL of plasma, while the sample was mixed on a vortex mixer. After centrifugation of the methanol/acetonitrile/water mixture at 2000xg for 10 min, the

Downloaded from dmd.aspetjournals.org at ASPET Journals on April 17, 2024

DMD Fast Forward. Published on November 5, 2007 as DOI: 10.1124/dmd.107.018416
This article has not been copyedited and formatted. The final version may differ from this version.

supernatant fraction was removed and saved, and the precipitate was resuspended and vortexed in acetonitrile/water (2:1, v/v). Following centrifugation, the supernatant fraction was removed and combined with the first supernatant. The combined supernatant fraction was evaporated to dryness under nitrogen and reconstituted in 0.2 mL of acetonitrile and water mixture (50:50, v/v). Following centrifugation at 2000xg for 5 min, a 50 μL portion was injected for HPLC analysis.

Each pooled fecal homogenate sample (1 mL) was extracted by addition of 3 mL of acetonitrile, while the sample was mixed on a vortex mixer. After centrifugation of the acetonitrile/water mixture at 2000xg for 10 min, the supernatant fraction was removed and saved, and the precipitate was resuspended and vortexed in acetonitrile/water (3:1, v/v). Following centrifugation, the supernatant was removed and combined with the first supernatant. The second extraction was repeated. This combined supernatant was evaporated to dryness under nitrogen and reconstituted in 0.5 mL acetonitrile and water mixture (50:50, v/v). Following centrifugation at 2000xg for 5 min, a portion of 20 μL was injected for HPLC analysis.

Determination of radioactivity and radioactivity profiles

Sample combustion was performed using a Packard Instruments Model A0387 sample oxidizer. The resulting $^{14}CO_2$ was trapped in Carbo-Sorb® (Packard Instruments) and mixed with Perma-Fluor (Packard Instruments) scintillation fluid and the radioactivity was quantified by liquid scintillation counting. Samples were analyzed for radioactivity in a Model LS 6500 liquid scintillation counter (Beckman Instruments) for 10 min.

Downloaded from dmd.aspetjournals.org at ASPET Journals on April 17, 2024

DMD Fast Forward. Published on November 5, 2007 as DOI: 10.1124/dmd.107.018416
This article has not been copyedited and formatted. The final version may differ from this version.

For quantification of radioactivity, HPLC effluent was collected in 0.25 min intervals using a Gilson Model 204 fraction collector. The plates were dried in an Automatic Environmental Speed Vac and counted for radioactivity for 10 min using a Packard TopCount NXT mictoplate scintillation and luminescence counter. Radiochromatograms were reconstructed from the TopCount data using Microsoft® Excel software.

Biotransformation profiles were prepared by plotting the CPM values against time-after-injection. For each injection, the average CPM value from a baseline section of 2-3 min in the chromatogram was subtracted from the CPM value of each fraction. Radioactivity peaks in the biotransformation profiles were reported as a percentage of the total radioactivity collected during the entire HPLC run.

Due to very low level of radioactivity, 12 and 24 h plasma samples of rats and dogs were not profiled.

LC/MS analysis

The extracts of pooled plasma, bile, urine and fecal samples, were analyzed by LC/MS using a Finnigan LCQ *Deca XP* ion trap mass spectrometer (ThermoFinnigan, San Jose, CA) and a Micromass Q-Tof Ultima mass spectrometer (Waters, Micromass, Boston, MA). The samples were analyzed in the positive electrospray ionization (ESI) mode. The mobile phase flow rate was 1 mL/min. The mobile phase was split before entering the mass spectrometry. The gradient used for LC/MS analysis was the same as for the HPLC analysis described above. Approximately 30% of the HPLC eluent was directed to the mass spectrometer through a divert valve set to divert the flow from 0-5 min. From 5 min until the end of the HPLC run, the effluent flow was directed to the mass spectrometer. The nitrogen gas flow rate, spray current, and voltages were adjusted to

Downloaded from dmd.aspetjournals.org at ASPET Journals on April 17, 2024

DMD Fast Forward. Published on November 5, 2007 as DOI: 10.1124/dmd.107.018416
This article has not been copyedited and formatted. The final version may differ from this version.

give maximum sensitivity for razaxaban. The capillary temperature used for analysis was 230°C for the LCQ. Exact mass measurements were obtained on a Micromass Q-Tof mass spectrometer that was equipped with a Lock-Spray and an ESI source. The desolvation temperature used for Q-Tof analysis was 300°C. The m/z 556.2771 of an infused 20 ng/μL leucine enkephalin solution was used as the Lock Mass. The Q-Tof was tuned to 18,000 resolution at half peak height using an insulin tuning solution, and was calibrated up to 1500 Da using a polyalanine calibration solution. The experimentally obtained masses were compared to their respective calculated values with an error of less than 5 mDa.

Incubations with hepatocytes

Hepatocytes from Spague-Dawley rats and beagle dogs were used. [^{14}C]Razaxaban (34.67 μCi/mg, 6.5 μL of 9.6 mM solution in methanol) was added to 1.25 mL portions of cell suspensions to a final concentration of 50 μM in Krebs-Henseleit buffer in open 22 mL glass vials. The cell concentrations were 4.8 and 3.1 million cells/mL from rats and dogs, respectively. The cell viability was 77 and 93% at the beginning of the incubations for rat and dog hepatocytes, respectively. The reaction vials were incubated with shaking (120 rpm) for 3 h in a 37°C chamber. The chamber was maintained under an oxygen/carbon dioxide (95/5) atmosphere. A 3-h incubation of [^{14}C]razaxaban (50 μM) in buffer served as a negative control. At the end of incubations, acetonitrile (2.5 mL) was added to each sample, and the mixtures were sonicated for 5 min in a Branson 5210 sonicator. The samples were centrifuged at 3000xg for 10 min. The supernatants were removed and aliquots were taken for counting of radioactivity. The radioactivity recoveries were >95% from these hepatocyte incubations. The supernatant was

Downloaded from dmd.aspetjournals.org at ASPET Journals on April 17, 2024

DMD Fast Forward. Published on November 5, 2007 as DOI: 10.1124/dmd.107.018416
This article has not been copyedited and formatted. The final version may differ from this version.

evaporated to near dryness under nitrogen. The residues were reconstituted in 0.2 mL of water/methanol (1:1, v/v) for LC/MS and LC/radiodetection.

Rat liver subcellular fractionation and in vitro incubations

The subcellular fractionations from livers of untreated male Sprague-Dawley rats was performed using a literature procedure with minor modifications (Lecureux et al., 1994). Briefly, approximately 1 g of the fresh rat liver tissue was immediately placed in 6 mL of ice-cold isotonic buffer containing 0.25 M sucrose in 10 mM Tris buffer at pH 7.2. Following homogenization of the tissue using a teflon homogenizer, the samples were subjected to differential centrifugation steps at 4°C. The homogenate was first centrifuged at 600xg for 10 min and cell debris containing nuclei, lysosomes, and tissue fragments were collected in the pellet. The supernatant was then centrifuged at 10,000xg for 10 min to precipitate mitochondria. Finally, the supernatant was centrifuged at 100,000xg for 60 min to separate the microsomes from the cytosol fraction. All pellet fractions were immediately placed on ice and 3 mL of the isotonic buffer was added to suspend the pellets. Protein concentration was determined using BCA protein assay kit (Pierce, Rockford, IL). The protein concentrations were 11.4, 8.35, 10.9, 4.85, and 6.39 mg/mL for homogenate, tissue debris, mitochondria, microsomes, and cytosol, respectively.

Incubation mixtures with rat liver fractions in a final volume of 1 mL contained 50 μL of 1 M phosphate pH 7.4, 5 μL of 9.6 mM [^{14}C]razaxaban, 0.1 mL of liver fractions (except 0.4 mL of cytosol), 0.1 mL of 1 mg/mL NADPH or NADH, and water. The protein concentrations were 1.1, 0.84, 1.1, 0.49, and 2.5 mg/mL for the homogenate, tissue

Downloaded from dmd.aspetjournals.org at ASPET Journals on April 17, 2024

DMD Fast Forward. Published on November 5, 2007 as DOI: 10.1124/dmd.107.018416
This article has not been copyedited and formatted. The final version may differ from this version.

debris, mitochondria, microsomes, and cytosol fractions, respectively. The reactions were initiated by adding NADPH or NADH.

Similar incubations were also performed with alcohol dehydrogenase and aldehyde dehydrogenase at a final protein concentration of 1 mg/mL replacing rat liver fractions. The control incubations were done without the addition of cofactors. The incubations were for 30 min at 37°C. Acetonitrile (2 mL) was added to the incubation mixture to terminate the reactions. The mixtures were centrifuged at 3000xg for 10 min and the supernatant were dried under a nitrogen stream before reconstituting in 0.2 mL of methanol:water (50:50, v/v). Aliquots of 50 μL were analyzed by HPLC and LC/MS.

Results

Mass balance

As shown in Table 1, the major route of excretion of [^{14}C]razaxaban was biliary in BDC rats and dogs during the 0-48 h collection, accounting for 34 and 44% of dose, respectively. The major route of excretion was fecal for intact rats and dogs during the 0-48 h collection, accounting for 88 and 76% of dose, respectively. Urinary excretion represented 3-5% of dose in intact rats and dogs, and but somewhat higher (11 and 13%) in surgical BDC rats and dogs. The radioactivity recovery was lower from BDC rats (63%) than from intact rats (>90%) during the limited 0-48 h sample collection. The radioactivity recovery was similar between two groups (BDC and intact) of dogs (approximately 80%).

Downloaded from dmd.aspetjournals.org at ASPET Journals on April 17, 2024

DMD Fast Forward. Published on November 5, 2007 as DOI: 10.1124/dmd.107.018416
This article has not been copyedited and formatted. The final version may differ from this version.

Metabolite identification

Metabolites were characterized by LC/MS/MS analysis, in some cases with comparison to synthetic standards. Metabolites were identified from plasma, urine, bile and feces of rats and dogs. Table 2 shows HPLC retention times, major fragmentation patterns, and chemical formula derived from accurate mass measurements. These m/z values are for C-12-containg metabolite species. The typical fragmentation for razaxaban and its metabolites was cleavage of the dimethylamine moiety (M-45). The glucuronidation sites for several glucuronide metabolites were not determined and glucuronidation could occur on multiple sites in the razaxaban molecule.

Parent. The parent compound had a molecular ion $[M+H]^+$ at m/z 529 and a major fragment ion at m/z 484 (Table 2). The chromatographic peak for the parent compound matched that of the synthetic standard.

*Metabolite **M1***. M1 had a molecular ion $[M+H]^+$ at m/z 531 and a major fragment ion at m/z 486, a two mass units higher than the parent compound (Table 2). Accurate mass measurement of M1 gave a molecular ion at m/z 531.1896 and a derived formula of C24H23N8O2F4 (1.6 mDa from the calculated value), suggesting that M1 resulted from reduction of razaxaban. M1 had the same HPLC retention time and fragmentation pattern as the synthetic standard. M1 was identified as dihydrorazaxaban.

*Metabolite **M2***. M2 had a molecular ion $[M+H]^+$ at m/z 707. LC/MS/MS analysis showed a product ion at m/z 531 that was the same as M1 (Table 2). The loss of 176 from the protonated molecular ion at m/z 707 suggested that M2 was a glucuronide of M1. Accurate mass measurement of M2 gave a molecular ion of 707.2181 and a derived formula of C30H31N8O8F4 (-2.0 mDa from the calculated value), confirming that M2 is

Downloaded from dmd.aspetjournals.org at ASPET Journals on April 17, 2024

DMD Fast Forward. Published on November 5, 2007 as DOI: 10.1124/dmd.107.018416
This article has not been copyedited and formatted. The final version may differ from this version.

a glucuronide conjugate of dihydrorazaxaban. The position of the glucuronic acid was not determined.

*Metabolite **M3***. M3 had a molecular ion $[M+H]^+$ at m/z 705. LC/MS/MS analysis showed a product ion at m/z 529. The loss of 176 from the protonated molecular ion at m/z 705 suggests that M3 was a glucuronide conjugate of razaxaban (Table 2). Accurate mass measurement of M3 gave a molecular ion of 705.2040 and a derived formula of C30H29N8O8F4 (-0.4 mDa from the calculated value), confirming that M3 is a direct glucuronide conjugate of razaxaban. The position for the glucuronic acid was not determined.

*Metabolite **M4***. M4 had a molecular ion $[M+H]^+$ at m/z 515 and a major fragment ion at m/z 484, which was consistent with demethylated razaxaban (loss of 14 mass units). Accurate mass measurement of M4 gave a molecular ion of 515.1572 and a derived formula of C23H19N8O2F4 (+0.5 mDa from the calculated value), suggesting that M4 resulted from *N*-demethylation of razaxaban. This metabolite had the same HPLC retention time and fragmentation pattern as the synthetic standard. M4 was identified as *N*-demethyl razaxaban.

*Metabolite **M5***. M5 had a molecular ion $[M+H]^+$ at m/z 517 and a major fragment ion at m/z 486, which was consistent with reductive isoxazole ring opening product of *N*-demethyl razaxaban (M4). This metabolite had the same HPLC retention time and fragmentation pattern as the synthetic standard. M5 was thus identified as *N*-demethyl dihydrorazaxaban.

*Metabolite **M7***. M7 had a molecular ion $[M+H]^+$ at m/z 502 and a major fragment at m/z 486, suggesting a deaminated product. Accurate mass measurement of M7 gave a

Downloaded from dmd.aspetjournals.org at ASPET Journals on April 17, 2024

DMD Fast Forward. Published on November 5, 2007 as DOI: 10.1124/dmd.107.018416
This article has not been copyedited and formatted. The final version may differ from this version.

molecular ion of 515.1572 and a derived formula of C22H16N7O3F4 (+2.9 mDa from the calculated value), supporting the structure proposed for M7. This metabolite had the same HPLC retention time and fragmentation pattern as the synthetic standard. M7 was presumably formed by deamination followed by reduction of razaxaban.

*Metabolite **M10***. M10 had a molecular ion $[M+H]^+$ at m/z 545 and a major fragment at m/z 484, which was consistent with an added 16 mass unit (oxygen) being cleaved off during the fragmentation and the oxygenation site was not on the isoxazole side of the molecule. Accurate mass measurement of M10 gave a molecular ion of 545.1671 and a derived formula of C24H21N8O3F4 (-0.2 mDa from the calculated value). These results suggested that M10 was an *N*-oxide of parent. This metabolite had the same HPLC retention time and fragmentation pattern as the synthetic standard. M10 was identified as razaxaban *N*-oxide.

*Metabolite **M11***. M11 had a molecular ion $[M+H]^+$ at m/z 721. LC/MS/MS analysis showed a product ion at m/z 545. The loss of 176 from the protonated molecular ion at m/z 721 suggests that M11 was a glucuronide of M10. Accurate mass measurement of M11 gave a molecular ion of 721.1988 (Table 2) and a derived formula of C30H29N8O9F4 (-0.6 mDa from the calculated value), confirming that M11 was a glucuronide of M10. The position of the glucuronic acid was not determined.

*Metabolite **M12***. M12 had a molecular ion $[M+H]^+$ at m/z 504 and a fragment ion at m/z 486, consistent with a deamination product of M1. Accurate mass measurement of M12 gave a molecular ion of 504.1416 and a derived formula of C22H18N7O3F4 (0.9 mDa from the calculated value), suggesting that M12 was a deamination product of M1. M12 was identified as deaminated and reduced dihydrorazaxaban.

Downloaded from dmd.aspetjournals.org at ASPET Journals on April 17, 2024

DMD Fast Forward. Published on November 5, 2007 as DOI: 10.1124/dmd.107.018416
This article has not been copyedited and formatted. The final version may differ from this version.

*Metabolite **M13***. M13 had a molecular ion $[M+H]^+$ at m/z 547 and a major fragment ion at m/z 486, consistent with the reductive ring opening of M10. Accurate mass measurement of M13 gave a molecular ion of 547.1834 and a derived formula of C24H23N8O3F4 (0.5 mDa from the calculated value), confirming that M13 was the reductive ring opening of M10. Metabolite M13 was identified as dihydrorazaxaban *N*-oxide.

*Metabolite **M14***. M14 had a molecular ion $[M+H]^+$ at m/z 723. LC/MS/MS analysis showed a product ion at m/z 547, indicating the loss of 176 from the protonated molecular ion of m/z 723. Accurate mass measurement of M14 gave a molecular ion of 723.2148 and a derived formula of C30H31N8O9F4 (-0.2 mDa from the calculated value). These results suggested that M14 was a glucuronide of M13, dihydrorazaxaban *N*-oxide glucuronide.

*Metabolite **M15***. M15 had a molecular ion $[M+H]^+$ at m/z 503, and a major fragment ion at m/z 486, suggesting di-demethylation of M1. Accurate mass measurement of M15 gave a molecular ion of 503.1581 and a derived formula of C22H19N8O2F4 (1.6 mDa from the calculated value), confirming that M15 was *N*,*N*-des-dimethyl dihydrorazaxaban.

Biotransformation profile in rats

[^{14}C]Razaxaban accounted for approximately 76% at 1 h and 69% of the radioactivity at 6 h in rat plasma. At 1 h, metabolites M1, M4, M7 and M12 accounted for 1, 1, 5 and 8% of the rat plasma radioactivity, respectively (Figure 3). These metabolites were not observed in 6 h rat plasma samples. In the 6 h plasma, there was an unidentified

Downloaded from dmd.aspetjournals.org at ASPET Journals on April 17, 2024

DMD Fast Forward. Published on November 5, 2007 as DOI: 10.1124/dmd.107.018416
This article has not been copyedited and formatted. The final version may differ from this version.

radioactive peak in the void volume (data not shown). This metabolite could result from further glucuronidation of a glucuronide metabolite.

Radioactivity distribution in rat urine, bile, and feces following oral administration is shown in Table 3. Metabolites M1, M2, M4, and M12 each represented <0.5% of dose in urine of intact rats (Figure 4). In urine (0-48 h) of BDC rats (Figure 5), the major metabolites were M1 and M4, which accounted for 3.3 and 1.3% of dose, respectively. M2 and M5 represented <1% of dose. The parent compound was a major component in rat urine.

In the 0-48 h bile from BDC rats, the parent compound accounted for 2% of the dose. M1 recovered in the bile (18% of dose) represented more than half of the biliary excretion (34% of dose). Other metabolites identified in the bile were M2, M4, M5, M10, and M12, each accounting for <4% of the dose. The extraction recovery of the rat feces homogenate ranged from 90-102%. From BDC rats, the 0-48 h fecal samples contained 18% of the dose. The parent compound accounted for 9.6% of the dose. M1 was the major metabolite and accounted for 4.3% of the dose (Figure 5). Metabolites M4 and M7 accounted for <1% of the dose. From intact rats, the 0-48 h feces samples contained 88% of the dose. The parent compound accounted for 7.0% of the dose. M1 was the major component, accounting for >64% of the dose (Figure 4). Other metabolites identified were M5, M7, and M12, each accounting for 1-7% of the dose. Parent and identified metabolites together accounted for >85% of radioactivity in urine, bile, and feces of rats.

Biotransformation profile in dogs

In dog plasma, 75-85% of the radioactivity represented parent drug at 1 and 6 h. At 1 h, metabolite M4 accounted for 7% and M7 for 8% of the plasma radioactivity (Figure 3)

Downloaded from dmd.aspetjournals.org at ASPET Journals on April 17, 2024

DMD Fast Forward. Published on November 5, 2007 as DOI: 10.1124/dmd.107.018416
This article has not been copyedited and formatted. The final version may differ from this version.

and at 6 h metabolite M4 and M7 accounted for 4 and 7%, respectively. Metabolite M1 accounted for 1% at 1 h and was not observed at 6 h in dog plasma.

Radioactivity distribution in dog urine, bile, and feces following oral administration is shown in Table 3. The dog urine samples (0-48 h) contained 13.6 and 5% of the dose from BDC and intact animals. Parent accounted for 2.0-2.8% of the dose. The eight metabolites M1, M2, M3, M4, M5, M7, M13 and M14 each accounted for 0.1-2.3% of dose, among which M1 and M4 were prominent metabolites (Figures 6 and 7). The extraction recovery of the feces homogenate ranged from 91 to 106% in dogs. From intact dogs, the pooled fecal samples (0-48 h) contained 75.5% of the dose. Parent was the major component which accounted for 46.8% of the dose. M1 was the major metabolite identified in the fecal sample (0-48 h) (Figure 6). From BDC dogs, the pooled fecal samples (0-48 h) contained 25% of the dose. The parent compound accounted for 7.5% of the dose. Among eight prominent metabolites (Figure 7) in BDC dog feces, M1 was a major metabolite (10.3% of dose). Metabolites M2, M7, M10 and M11 were less than 1% of dose.

The 0-48 h bile samples from BDC dogs contained 44% of the dose. The parent compound accounted for 6.6% of the dose. The metabolites identified in the bile were M1, M2, M3, M4, M5, M7, M10, M11, M12, and M13, among which M1, M4, M10, and M11 were prominent metabolites, each representing >3.1% of dose (Figure 7). Parent and identified metabolites together accounted for >88% of radioactivity in urine, bile, and feces of dogs. The *N*-oxide metabolite M10 was a significant metabolite in dog bile (5.5% of dose) but not in the feces.

Downloaded from dmd.aspetjournals.org at ASPET Journals on April 17, 2024

DMD Fast Forward. Published on November 5, 2007 as DOI: 10.1124/dmd.107.018416
This article has not been copyedited and formatted. The final version may differ from this version.

Metabolite profile in rat liver tissue

The metabolite profile of [^{14}C]razaxaban in rat liver tissues at different time points are shown in Figure 8. Metabolites M1 and M5 were the major metabolites in the liver homogenates at 1, 6, and 12 h following a single oral administration of [^{14}C]razaxaban. In addition to M1 and M5, minor metabolites M10 and M12 were also detected but no parent was found.

Metabolite profile in hepatocyte incubations

The metabolite profiles of [^{14}C]razaxaban in incubations with hepatocytes of rats and dogs are shown in Figure 9. M1 was the major metabolite in the fresh rat hepatocytes and a relatively minor metabolite in cryopreserved dog hepatocytes. It is not known if cryopreservation affected the M1 formation activity in dog hepatocytes. In addition to M1, metabolites M2, M3, M4, M5, M10, M12, and M13 were also found in rat hepatocytes, some of these metabolites were also produced in dog hepatocytes in lower amounts.

Enzyme activity of M1 formation in rat liver fractions

Table 4 shows the activities for M1 formation in different rat liver fractions. The incubations without addition of NADH or NADPH did not show any M1 formation activity. Incubations in the presence of NADH showed that the liver homogenate, cell debris, and cytosol had the highest isoxazole reduction activity to form M1. A relatively lower level of M1 was formed in mitochondria and microsomal fractions. Incubations in the presence of NADPH with these liver fractions showed less than 20% of M1 formation activities compared the incubations in the presence of NADH. Alcohol dehydrogenase

Downloaded from dmd.aspetjournals.org at ASPET Journals on April 17, 2024

DMD Fast Forward. Published on November 5, 2007 as DOI: 10.1124/dmd.107.018416
This article has not been copyedited and formatted. The final version may differ from this version.

from equine livers and aldehyde dehydrogenase from yeast did not show any formation of M1.

Discussion

Several marketed agents, including the anticonvulsant zonisamide, antipsychotic risperidone and iloperidone, and anti-inflammatory valdecoxib contain the 1,2-isoxazole ring structure. All of these compounds have been demonstrated to undergo reductive metabolism resulting in the cleavage of N-O bond leading to imine intermediates (Stiff et al., 1992; Mannens et al., 1993; Mutlib et al., 1995; Yuan et al., 2002). However, the imine intermediates themselves have never been isolated due to their rapid hydrolysis in aqueous media to ketones. The antipsychotic ziprasidone, containing a 1,2-benzisothiazole ring structure, also undergoes similar reductive metabolism resulting in the cleavage of N-S bond to form an amidine intermediate. This amidine intermediate was not detected in vivo in preclinical species due either to instability or rapid metabolism to a methylthioether by methylation with S-thiomethyl transferases (Prakash et al., 1997, 2000). In this study, we reported that the 1,2-benzisoxazole ring structure of razaxaban undergoes a similar reductive metabolism to form a stable benzamidine metabolite both in rats and dogs and in hepatocyte incubations.

[^{14}C]Razaxaban was extensively metabolized in BDC rats and dogs, primarily by reductive isoxazole ring opening. The metabolites were primarily excreted into bile. Among the twelve metabolites identified, M1, M2 (glucuronide of M1), M5 (*N*-demethyl M1), M12 (*N*,*N*-di-des-methyl deamination of M1), M13 (*N*-oxide of M1), M14 (glucuronide of M13), and M15 (*N*,*N*-di-des-methyl M1) all had a benzamidine structure resulting from isoxazole-ring reduction. Other metabolites were minor, including M3

Downloaded from dmd.aspetjournals.org at ASPET Journals on April 17, 2024

DMD Fast Forward. Published on November 5, 2007 as DOI: 10.1124/dmd.107.018416
This article has not been copyedited and formatted. The final version may differ from this version.

(glucuronide of parent), M4 (*N*-demethyl M1), M7 (deamination followed by reduction of the parent), M9 (glucuronide of M4), M10 (*N*-oxide of parent), and M11 (glucuronide of M10). In addition, several glucuronide metabolites were observed in the bile samples from BDC rats and dogs, but not in the feces from the intact rats and dogs, suggesting that they were hydrolyzed by gut microflora. Similarly, razaxaban *N*-oxide was a prominent metabolite in dog bile but not feces. The *N*-oxide was presumably reduced back to the parent before being excreted in feces. There seemed to be more *N*-oxide metabolites formed in dogs than in rats in both *in vivo* and in hepatocyte incubations.

M1 could be formed by enzymes in the liver or other organs or pre-systemically by intestinal microflora. There are several lines of evidence that support the formation of M1 in the liver including: 1) The presence of M1 in bile and urine of BDC dogs following oral administration of razaxaban, 2) the detection of M1 as the major metabolite in rat liver samples collected at 1, 6, and 12 h after a single oral dose of razaxaban, and 3) the formation of M1 as the major metabolite in incubations in hepatocytes of rats and dogs. The observation of M1 in feces of BDC rats and dogs suggested that M1 was also formed in fecal contents, presumably through reduction by gut microflora or was directly excreted into the intestines.

The enzymes responsible for reductive metabolism of other isoxazole ring structures have been described in the literature. The reductive metabolism of zonisamide can be catalyzed by several enzymes, especially CYP3A4 (Nakasa et al., 1993) and aldehyde oxidase (Sugihara et al., 1996), as well as intestinal bacteria (Kitamura et al., 1997). The reduction of the isoxazole ring of risperidone was mainly due to gut microflora (Mannens et al., 1993). The N-O bonds in 3-(indole-1-yl)-1,2-benzisoxazoles were reported to be

Downloaded from dmd.aspetjournals.org at ASPET Journals on April 17, 2024

DMD Fast Forward. Published on November 5, 2007 as DOI: 10.1124/dmd.107.018416
This article has not been copyedited and formatted. The final version may differ from this version.

reduced followed by *N*-dearylation via CYP3A4 in rat liver microsomes under anaerobic conditions (Tschirret-Guth and Wood, 2003). The reduction of the N-S bond in ziprasidone appeared to be catalyzed by aldehyde oxidase since menadione, a specific aldehyde oxidase inhibitor, abolished >70% of the formation of dihydroziprasidone (Miao et al., 2005). The 1,2-isoxazole ring opening reaction of razaxaban was not catalyzed by equine liver alcohol dehydrogenase, nor by yeast aldehyde dehydrogenase. Our preliminary results suggested that a NADH-dependent cytosolic enzyme catalyzes the isoxazole reduction of razaxaban in rat liver although the exact enzyme responsible for this reaction is not known. The enzyme activity observed in the cell debris could be due to a membrane bound activity, but is more likely due to contamination by the cytosolic enzymes.

Tschirret-Guth and Wood (2003) studied the isoxazole ring-substitution effects on the reduction of the N-O bond of 1,2-benzisoxazole. Addition of electro-withdrawing groups (Cl^-, $CH_3SO_2^-$) at the 6-position of the 1,2-benzisoxazole ring cause an increase in the rate of reduction. The proposed mechanism suggested that initial electron transfer to the 1,2-isoxazole ring would yield a radical anion with nitrogen bearing the negative charge and a benzylic radical. Homolysis at the N-O bond would yield a phenoxy radical and the imine. Reductive ring opening of the 1,2-isoxazole heterocycles appeared to require a specific substitution pattern. 3-Methyl-5-alkyl substituted 1,2-isoxazole ABT-418 (Martin et al., 1997) and 5-methylisoxazole 3-carboxamides D2624 and AG7088 (Rodrigues et al., 1995; Zhang et al., 2001) and 3,5-dimethylisoxazole-4-carboxamide (3-methylleflunomide) underwent extensive methyl hydroxylation and no reductive ring opening was reported for these systems. However, 5-methylisoxazole-4-carboxamide

Downloaded from dmd.aspetjournals.org at ASPET Journals on April 17, 2024

DMD Fast Forward. Published on November 5, 2007 as DOI: 10.1124/dmd.107.018416
This article has not been copyedited and formatted. The final version may differ from this version.

(leflunomide) underwent extensive reductive cleavage of the N-O bond (Kalgutkar et al., 2003). It is not know how the amino-substitute in the benzisoxazole of razaxaban affected the N-O bond reduction compared to the reduction of other isoxazole-containing compounds.

In summary, [^{14}C]razaxaban was extensively metabolized in rats and dogs. Isoxazole reduction forming a stable benzamidine (M1) was the major metabolic clearance pathway for razaxaban. This reduction reaction was catalyzed by NADH-dependent cytosolic enzyme(s) in the liver and possibly by intestinal microflora.

Acknowledgements. We would like to thank Drs. W. Griffith Humphreys and Scott Grossman for critical review of the manuscript.

Downloaded from dmd.aspetjournals.org at ASPET Journals on April 17, 2024

DMD Fast Forward. Published on November 5, 2007 as DOI: 10.1124/dmd.107.018416
This article has not been copyedited and formatted. The final version may differ from this version.

References

Barrett JS, Davidson AF, Jiao QT, Mosqueda-Garcia R, Kornhauser DM, Gangrade NK, Jona JA, and Pieniaszek HJ Jr (2001) The Effect of food, formulation, and dosing duration on the pharmacokinetics of DPC423, a potent factor Xa inhibitor. *J Clin Pharmacol* **41** (9): 42.

Dalvie DK, Kalgutkar AS, Khojesth-Bakht SC, Obach RS, and O'Donnell JP (2002) Biotransformation reactions of five-membered aromatic heterocyclic rings. *Chem Res Toxicol* **15:** 269–299.

Jin F and Confalone PN (2000) Palladium-catalyzed cyanation reactions of aryl chlorides. *Tetrah Lett* **41**: 3271-3273.

Kitamura S, Sugihara K, Kuwasako M, and Tatsumi K (1997) The role of mammalian intestinal bacteria in the reductive metabolism of zonisamide. *J Pharm Pharmacol* **49:** 253–256.

Kitamura S and Tatsumi K (1984) Reduction of tertiary amine N-oxides by liver preparations: function of aldehyde oxidase as a major N-oxide reductase. *Biochem Biophys Res Commun* **121:** 749–754.

Lam PYS, Clark CG, Li R, Pinto DJ, Orwat MJ, Galemmo RA, Fevig JM, Teleha CA, Alexander RA, Smallwood AM, Rossi KA, Wright MR, Bai SA, He K, Luettgen JM, Wong PC, Knabb RM, and Wexler RR (2003) Structure-based design of novel guanidine/benzamidine mimics: Potent and orally bioavailable factor Xa inhibitors as novel anticoagulants. *J Med Chem* **46***:* 4405-4418.

Leadley, R. J., Jr. (2001) Coagulation factor Xa inhibition: Biological background and rationale. *Curr Top Med Chem* **1:** 151-159.

Lecureux LW, and Wattenberg BW (1994) The regulated degradation of a 3-hydroxy-3-methylglutaryl-coenzyme A reductase receptor construct occurs in the endoplasmic reticulum. *J Cell Sci* **107:** 2635-2642.

Mannens G, Huang ML, Meuldermans W, Hendrickx J, Woestenborghs R, and Heykants J (1993) Absorption, metabolism and excretion of risperidone in humans. *Drug Metab Dispos* **21:** 1134–1140.

Mann KG, Butenas S, and Brummel K (2003) The dynamics of thrombin formation. *Arterioscler Thromb Vasc Biol* **23***:* 17-25.

Mutlib AE, Strupczewski JT, and Chesson SM (1995) Application of hyphenated LC/NMR and LC/MS techniques in rapid identification of *in vitro* and *in vivo* metabolites of iloperidone. *Drug Metab Dispos* **23:** 951–964.

Nakasa H, Komiya M, Ohmori S, Rikihisa T, Kiuchi M, and Kitada M (1993) Characterization of human liver microsomal cytochrome P-450 involved in the reductive metabolism of zonisamide. *Mol Pharmacol* **44:** 216–221.

Downloaded from dmd.aspetjournals.org at ASPET Journals on April 17, 2024

DMD Fast Forward. Published on November 5, 2007 as DOI: 10.1124/dmd.107.018416
This article has not been copyedited and formatted. The final version may differ from this version.

Pinto DJ, Orwat MJ, Wang S, Fevig JM, Quan ML, Amparo E, Cacciola J, Rossi KA, Alexander RS, Wong PC, Knabb RM, Luettgen JM, Aungst BJ, Li L, Wright M, Jona JA, Wexler RR, and Lam PYS (2001) The discovery of 1-[3-aminomethyl)phenyl]-*N*-[3-fluoro-2'-(methylsulfonyl)-1,1'-biphenyl-4-yl]-3-(trifluoromethyl)-1*H*-pyrazole-5-carboxamide (DPC423), a highly potent, selective and orally bioavailable inhibitor of blood coagulation factor Xa. *J Med Chem* ***44****:* 566-578.

Prakash C, Kamel A, and Cui D (1997a) Identification of novel benzisothiazole cleaved products of ziprasidone. *Drug Metab Dispos* **25:** 897–901.

Prakash C, Kamel A, Cui D, Whalen R, Miceli J, and Tweedie D (2000) Identification of the major human liver cytochrome P450 isoform responsible for the formation of the primary metabolites of ziprasidone and prediction of possible drug interactions. *Br J Clin Pharmacol* **49 (Suppl 1):** 35S–42S.

Prakash C, Kamel A, Gummerus J, and Wilner K (1997b) Metabolism and excretion of the antipsychotic drug, ziprasidone, in humans. *Drug Metab Dispos* **25:** 863–872.

Quan ML, Lam PYS, Han Q, Pinto DJP, He MY, Li R, Ellis CD, Clark CG, Teleha CA, Sun JH, Alexander RS, Bai S, Luttgen JM, Knabb RM, Wang PC, and Wexler RR (2005) Discovery of 1-(3'-Aminobenzisoxazol-5'-yl)-3-trifluoromethyl-*N*-[2-fluoro-4- [(2'-dimethylaminomethyl)imidazol-1-yl]phenyl]-1*H*-pyrazole-5-carboxyamide Hydrochloride (Razaxaban), a Highly Potent, Selective, and Orally Bioavailable Factor Xa Inhibitor. *J Med Chem* **48:** 1729-1744.

Samama MM (2002) Synthetic direct and indirect factor Xa inhibitors. *Thromb Res* **106***:* V267-V273.

Stein P D, Grandison D, and Hua TA (1994) Therapeutic level of anticoagulation with warfarin in patients with mechanical prosthetic heart valves; review of literature and recommendations based on internal normalized ratio. *Postgrad Med J* **70** (Suppl. 1): S72-S83.

Stiff DD, Robicheau JT, and Zemaitis MA (1992) Reductive metabolism of the anticonvulsant agent zonisamide, a 1,2-benzisoxazole derivative. *Drug Metab Dispos* **18:** 888–894.

Sugihara K, Kitamura S, and Tatsumi K (1996) Involvement of mammalian liver cytosols and aldehyde oxidase in reductive metabolism of zonisamide. *Drug Metab Dispos* **24:** 199–202.

Tatsumi K and Ishigai (1987) Oxime-metabolizing activity of liver aldehyde oxidase. *Arch Biochem Biophys* **247:** 289–293.

Downloaded from dmd.aspetjournals.org at ASPET Journals on April 17, 2024

DMD Fast Forward. Published on November 5, 2007 as DOI: 10.1124/dmd.107.018416
This article has not been copyedited and formatted. The final version may differ from this version.

Tschirret-Guth R and Wood HB (2003) Substituent effect on the reductive dearylation of 3-(indol-1-yl)-1,2-benzisooxazoles by rat liver microsomes. *Drug Metab Dispos* **31:** 999–1004.

Walenga JM, Jeske WP, and Hoppensteadt D, and Fareed, J (2003) Factor Xa inhibitors: Today and beyond. *Curr Opin Invest Drugs **4*** **(3):** 272-281.

Wong PC, Crain EJ, Watson CA, Zaspel AM, Wright MR, Lam PYS, Pinto DJ, Wexler RR, and Knabb RM (2002) Nonpeptide factor Xa inhibitors III: Effects of DPC423, an orally-active pyrazole antithrombotic agent, on arterial thrombosis in rabbits. *J Pharmacol Exp Ther* **303***:* 993-1000.

Wong PC, Pinto DJ, and Knabb RM (2002) Nonpeptide factor Xa inhibitors: DPC423, a highly potent and orally bioavailable pyrazole antithrombotic agent. *Cardiovasc Drug Rev **20*** **(2)**: 137-152.

Wong PC, Crain EJ, Watson CA, Wexler RR, Lam PY, Quan ML, and Knabb RM (2007) Razaxaban, a direct factor Xa inhibitor, in combination with aspirin and/or clopidogrel improves low-dose antithrombotic activity without enhancing bleeding liability in rabbits. *J Thromb Thrombolysis* **24(1)**:43-51.

Downloaded from dmd.aspetjournals.org at ASPET Journals on April 17, 2024

DMD Fast Forward. Published on November 5, 2007 as DOI: 10.1124/dmd.107.018416
This article has not been copyedited and formatted. The final version may differ from this version.

Footnote:

GLS Current Address**:**

Amgen, Department of Pharmacokinetics and Drug Metabolism

One Amgen Center Drive

Thousand Oaks, CA 91320

gskiles@amgen.com

Downloaded from dmd.aspetjournals.org at ASPET Journals on April 17, 2024

DMD Fast Forward. Published on November 5, 2007 as DOI: 10.1124/dmd.107.018416
This article has not been copyedited and formatted. The final version may differ from this version.

Legends for Figures

Figure 1. Proposed metabolic pathways of razaxaban in rats and dogs.

Figure 2. Synthetic scheme for [^{14}C]razaxaban (BMS-561389).

Figure 3. Radiochromatograms of pooled plasma samples (1 h) after an oral administration of [^{14}C]razaxaban to dogs (30 μCi/20 mg/kg) and rats (100 μCi/300 mg/kg).

Figure 4. Radiochromatograms of pooled urine and fecal samples (0-48 h) after oral administration of [^{14}C]razaxaban to intact rats at 100 μCi/300 mg/kg.

Figure 5. Radiochromatograms of pooled urine, bile and fecal samples (0-48 h) after oral administration of [^{14}C]razaxaban to BDC rats at 100 μCi/300 mg/kg.

Figure 6. Radiochromatograms of pooled urine and fecal samples (0-48 h) after an oral administration of [^{14}C]razaxaban to intact dogs at 30 μCi/20 mg/kg.

Figure 7. Radiochromatograms of pooled urine, bile and fecal samples (0-48 h) after oral administration of [^{14}C]razaxaban to BDC dogs at 30 μCi/20 mg/kg.

Figure 8. Radiochromatograms of liver homogenate at 1, 6, and 24 h of rats after oral administration of [^{14}C]razaxaban at 100 μCi/300 mg/kg.

Figure 9. Metabolite profiles of [^{14}C]razaxaban in incubations in fresh rat hepatocytes and cryopreserved dog hepatocytes. The peak at 26 min is razaxaban *N*-oxide in the buffer incubation.

Downloaded from dmd.aspetjournals.org at ASPET Journals on April 17, 2024

DMD Fast Forward. Published on November 5, 2007 as DOI: 10.1124/dmd.107.018416
This article has not been copyedited and formatted. The final version may differ from this version.

Table 1. Percent of the radioactive dose recovered in urine, bile and feces during 0-48 h collections following an oral dose of [^{14}C]razaxaban to rats and dogs

Species	**Number of Animals**	**Dose[a] (mg/kg)**	**Matrix[b]**	**Average Recovery (% of dose)**
BDC Rat	3	300	Urine Feces Bile Total	11.0 18.1 34.2 63
Intact Rat	3	300	Urine Feces Total	3.4 88.1 91.5
BDC Dog	2	20	Urine Feces Bile Total	13.6 25.0 43.9 84
Intact Dog	2	20	Urine Feces Total	5.0 75.5 79.5

[a] Dose was prepared as suspension in 0.5% methycellulose at 25 mg/mL.

[b] Collected 0-48 h post dose.

Downloaded from dmd.aspetjournals.org at ASPET Journals on April 17, 2024

DMD Fast Forward. Published on November 5, 2007 as DOI: 10.1124/dmd.107.018416
This article has not been copyedited and formatted. The final version may differ from this version.

Table 2. Identification of [^{14}C]razaxaban metabolites in rats and dogs

Metab	**HPLC Time (min)**	**$[M+H]^+$ & fragment ions (m/z)**	**Accurate mass & molecular formula**	**Identity**
Parent	48.3	529; 484, 467, 457	Not determined	Razaxaban
M1	28.5	531; 486, 469, 457	531.1896 +0.0016 $C_{24}H_{23}N_8O_2F_4$	Dihydro razaxaban
M2	16	707; 531	707.2181 -0.0020 $C_{30}H_{31}N_8O_8F_4$	Dihydro razaxaban glucuronide
M3	24.8	705; 529	705.2040 -0.004 $C_{30}H_{29}N_8O_8F_4$	Razaxaban glucuronide
M4	41	515; 484, 472, 467, 457	515.1572 +0.005 $C_{23}H_{19}N_8O_2F_4$	*N*-Demethyl razaxaban
M5	23.5	517; 486	Not determined	*N*-Demethyl dihydro razaxaban
M7	39	502; 484, 467, 457, 295, 253, 190	502.1280 +0.0029 $C_{22}H_{16}N_7O_3F_4$	Deaminated razaxaban
M10	26	545; 484, 467, 457	545.1671 -0.002 $C_{24}H_{21}N_8O_3F_4$	Razaxaban *N*-oxide
M11	18.8	721; 676, 545, 500, 312	721.1988 -0.006 $C_{30}H_{29}N_8O_9F_4$	Razaxaban *N*-oxide glucuronide
M12	21.8	504; 486, 475, 469, 457	504.1416 +0.009 $C_{22}H_{18}N_7O_3F_4$	Deaminated dihydro razaxaban
M13	12.3	547; 502, 486, 469, 325	547.1834 +0.005 $C_{24}H_{23}N_8O_3F_4$	Dihydro razaxaban *N*-oxide
M14	9.5	723; 663, 547, 502, 486	723.2148 -.0002 $C_{30}H_{31}N_8O_9F_4$	Dihydro razaxaban *N*-oxide glucuronide
M15	37.8	503; 431, 433	503.1581 -0.0016 $C_{22}H_{19}N_8O_2F_4$	*N*,*N*-des-dimethyl dihydro razaxaban

Downloaded from dmd.aspetjournals.org at ASPET Journals on April 17, 2024

DMD Fast Forward. Published on November 5, 2007 as DOI: 10.1124/dmd.107.018416
This article has not been copyedited and formatted. The final version may differ from this version.

Table 3. Percent distribution of radioactive metabolites in pooled urine, bile and feces from rats and dogs after oral doses of [^{14}C]razaxaban

Metabolite radioactivity distribution (% of dose)										
Metab. ID	**BDC Rat (0-48 h)**			**Intact Rat (0-48 h)**		**Intact Dog (0-48 h)**		**BDC Dog (0-48 h)**		
	urine	bile	feces	urine	feces	urine	feces	urine	bile	feces
M1	3.3	18.1	4.3	0.48	63.4	0.85	11.3	2.2	7.4	10.3
M2	0.33	2.1	ND	0.03	0.05	0.35	2.3	1.4	1.3	0.25
M3	ND[b]	ND	ND	ND	ND	0.30	ND	0.7	1.3	ND
M4	1.3	4.1	0.54	0.48	ND	0.60	1.5	2.3	8.3	1.1
M5	0.99	2.4	ND	0.03	7.0	0.20	3.8	1.3	2.2	1.5
M7	ND	ND	0.9	ND	0.88	0.15	1.5	0.4	2.2	0.25
M10	ND	0.34	ND	ND	ND	ND	0.75	0.14	5.3	0.25
M11	ND	ND	0.05	ND	ND	ND	ND	0.14	3.1	0.25
M12	ND	1.0	0.10	0.03	3.5	ND	1.5	0.28	0.44	1.3
M13	0.11	0.10	ND	ND	ND	0.10	ND	0.68	0.44	ND
M14	ND	ND	ND	0.10	ND	0.10	ND	0.41	ND	ND
Parent	3.8	2.0	9.6	2.1	7.0	2.0	46.8	2.8	6.6	7.5
Others[a]	1.2	4.1	2.7	0.1	6.3	0.30	6.0	0.85	5.3	2.3
Total	11.0	34.2	18.1	3.4	88.1	5.0	75.5	13.6	43.9	25.0

[a] Radioactivity distributed among many small peaks each representing <0.03%.

[b] ND - Not detected.

M15 was a trace metabolite and detected by LC/MS in dog bile.

Downloaded from dmd.aspetjournals.org at ASPET Journals on April 17, 2024

DMD Fast Forward. Published on November 5, 2007 as DOI: 10.1124/dmd.107.018416
This article has not been copyedited and formatted. The final version may differ from this version.

Table 4. NADH-dependent M1 formation activities in rat liver fractions

Rat Liver Fractions	**Cofactors**	**M1 activity (pmol/mg/min)**
Liver Homogenate	NADPH	69.9
	NADH	449
Cell debris	NADPH	0.0
	NADH	479
Mitochondria	NADPH	0.0
	NADH	43.9
Microsomes	NADPH	33.0
	NADH	66.0
Cytosol	NADPH	50.0
	NADH	225

Downloaded from dmd.aspetjournals.org at ASPET Journals on April 17, 2024

Fig 1

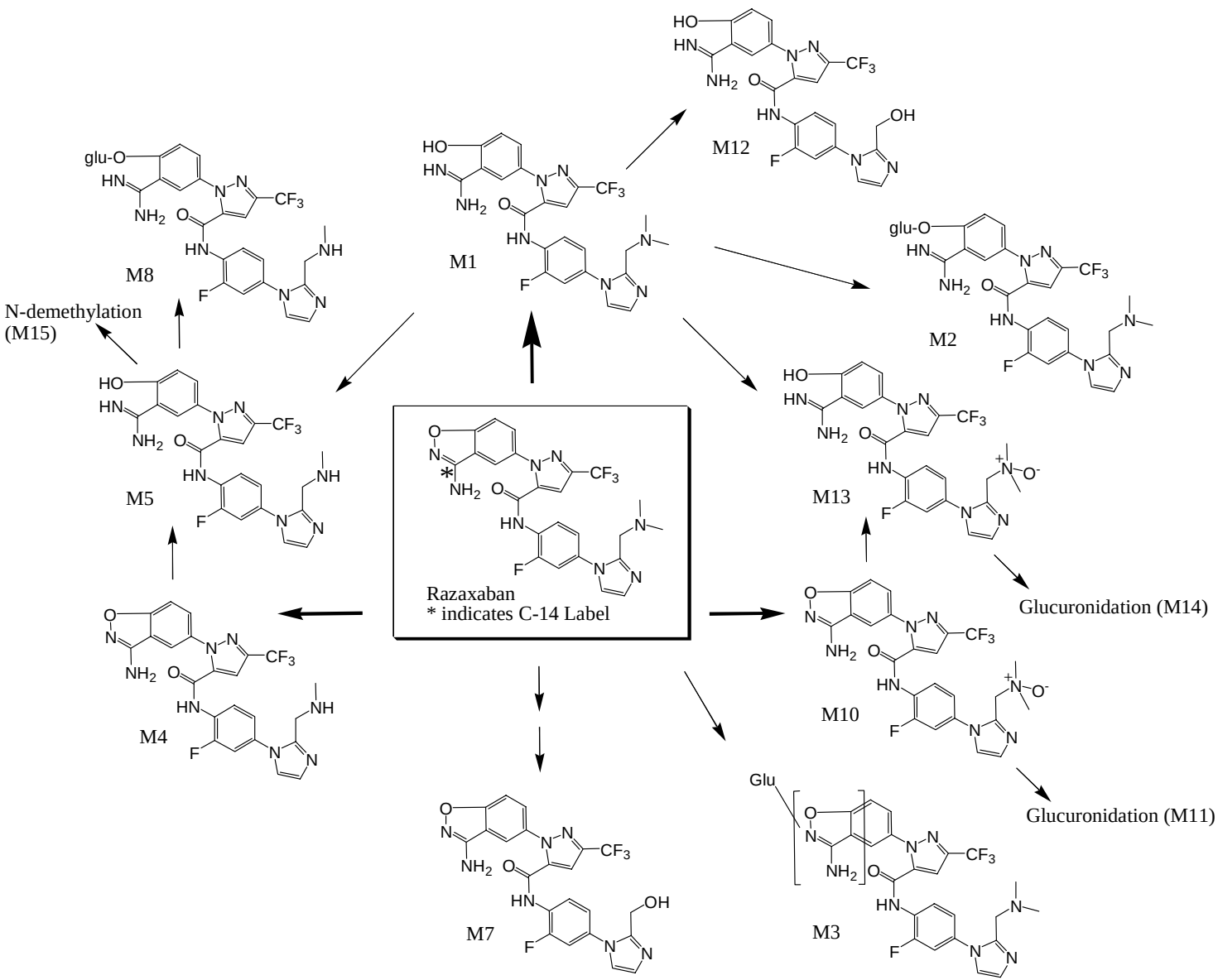

DMD Fast Forward. Published on November 5, 2007 as DOI: 10.1124/dmd.107.018416
This article has not been copyedited and formatted. The final version may differ from this version.

Downloaded from dmd.aspetjournals.org at ASPET Journals on April 17, 2024

DMD Fast Forward. Published on November 5, 2007 as DOI: 10.1124/dmd.107.018416
This article has not been copyedited and formatted. The final version may differ from this version.

Figure 2

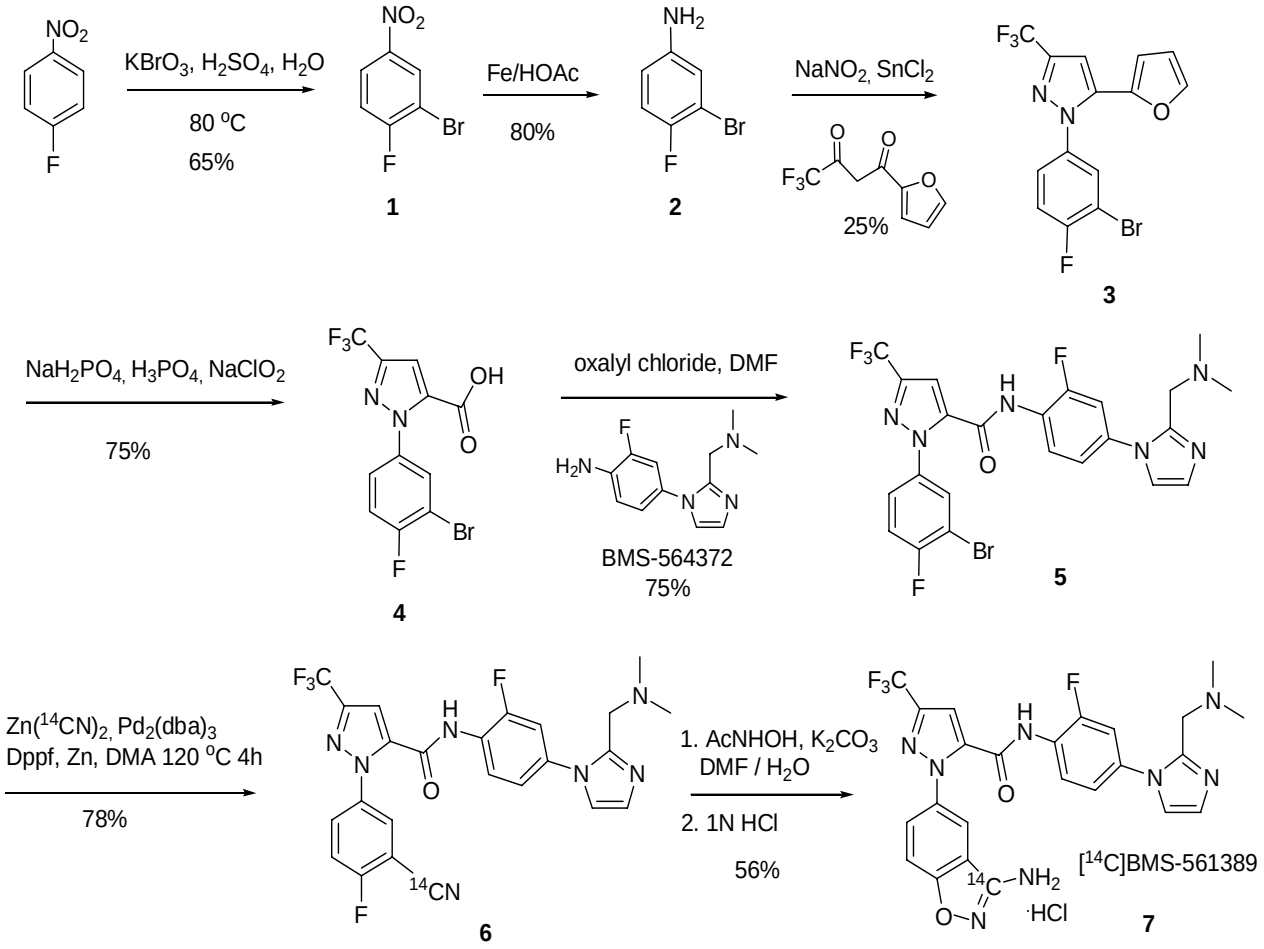

Downloaded from dmd.aspetjournals.org at ASPET Journals on April 17, 2024

DMD Fast Forward. Published on November 5, 2007 as DOI: 10.1124/dmd.107.018416
This article has not been copyedited and formatted. The final version may differ from this version.

Figure 3

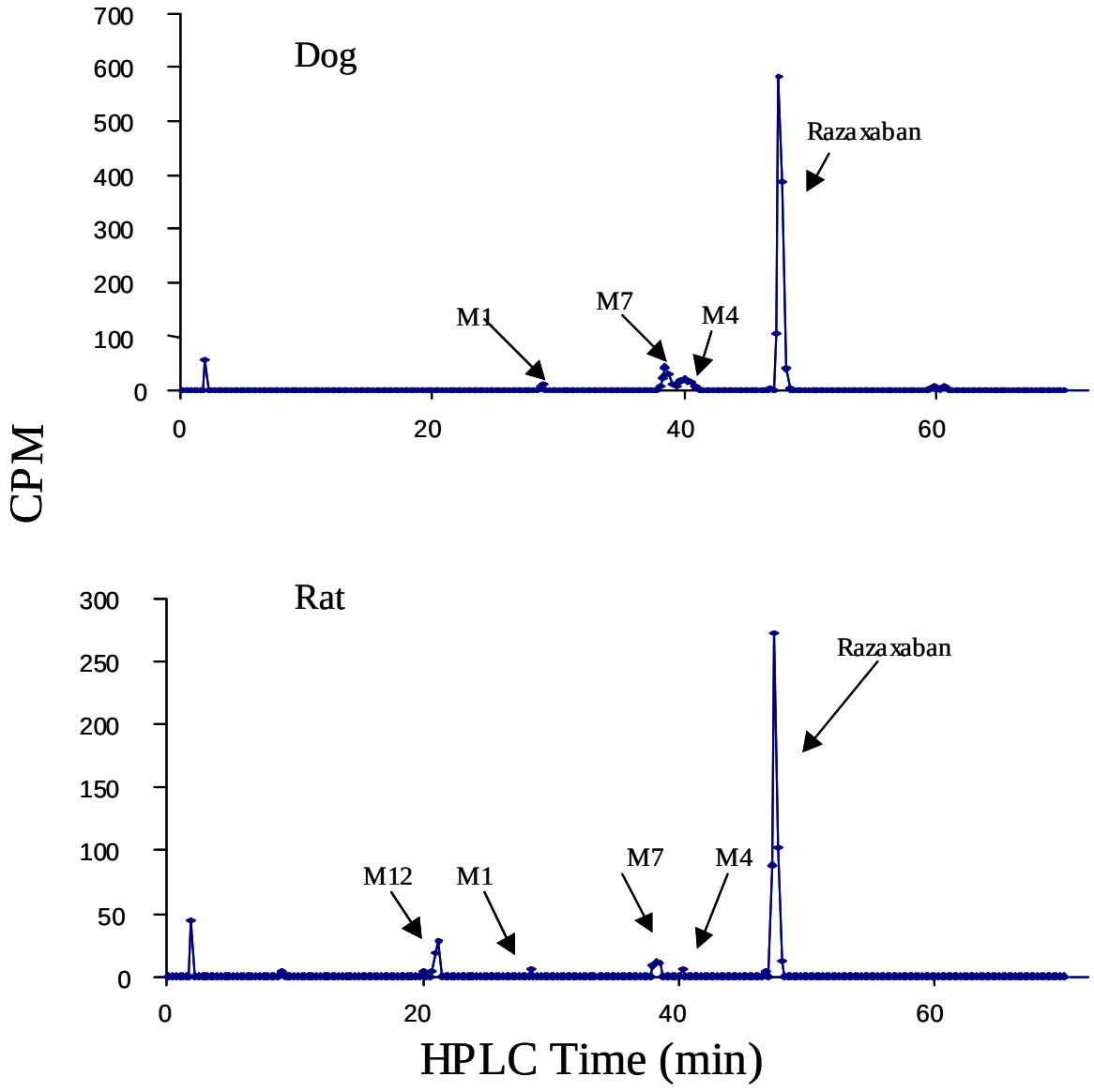

Downloaded from dmd.aspetjournals.org at ASPET Journals on April 17, 2024

DMD Fast Forward. Published on November 5, 2007 as DOI: 10.1124/dmd.107.018416
This article has not been copyedited and formatted. The final version may differ from this version.

Figure 4

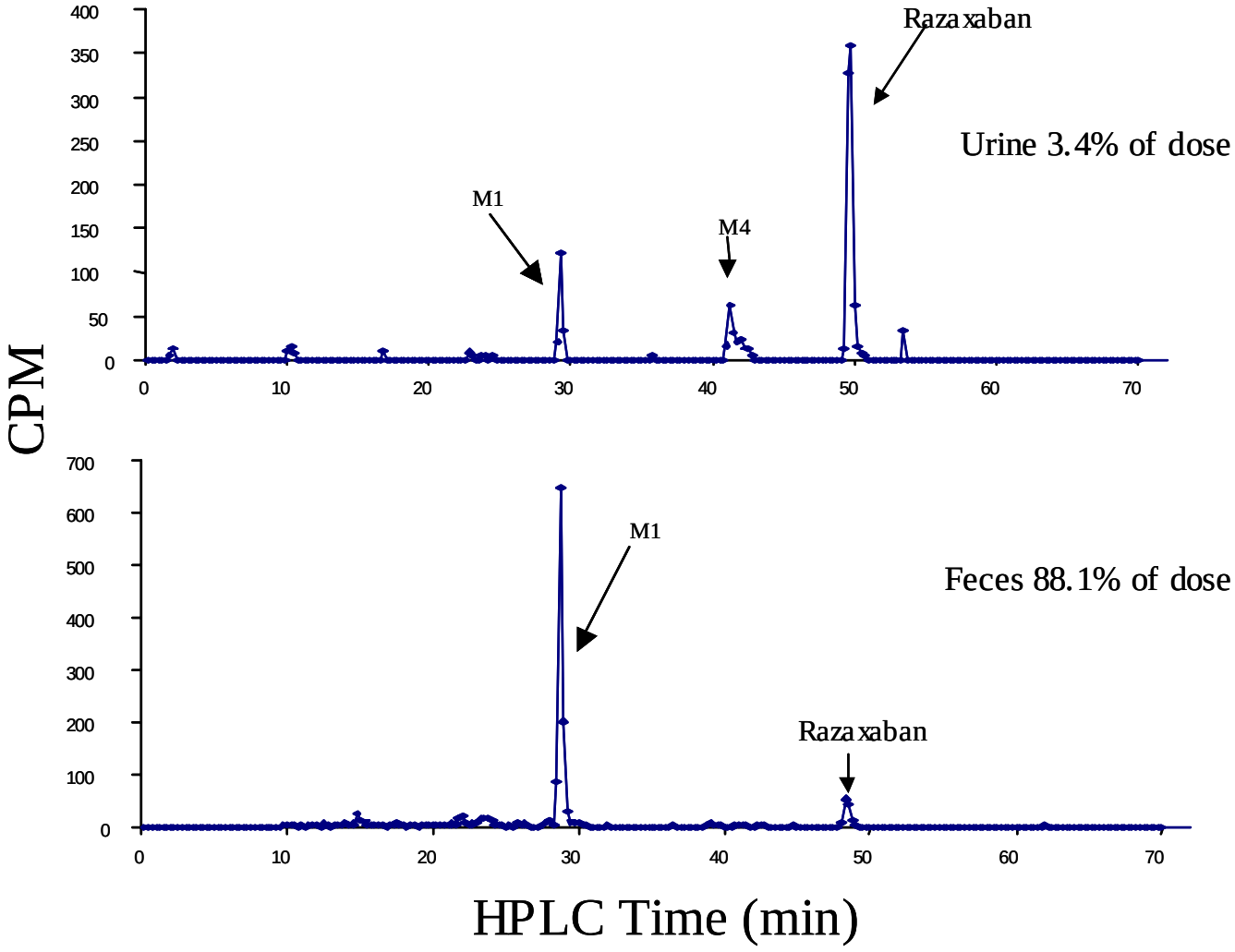

Downloaded from dmd.aspetjournals.org at ASPET Journals on April 17, 2024

DMD Fast Forward. Published on November 5, 2007 as DOI: 10.1124/dmd.107.018416
This article has not been copyedited and formatted. The final version may differ from this version.

Figure 5

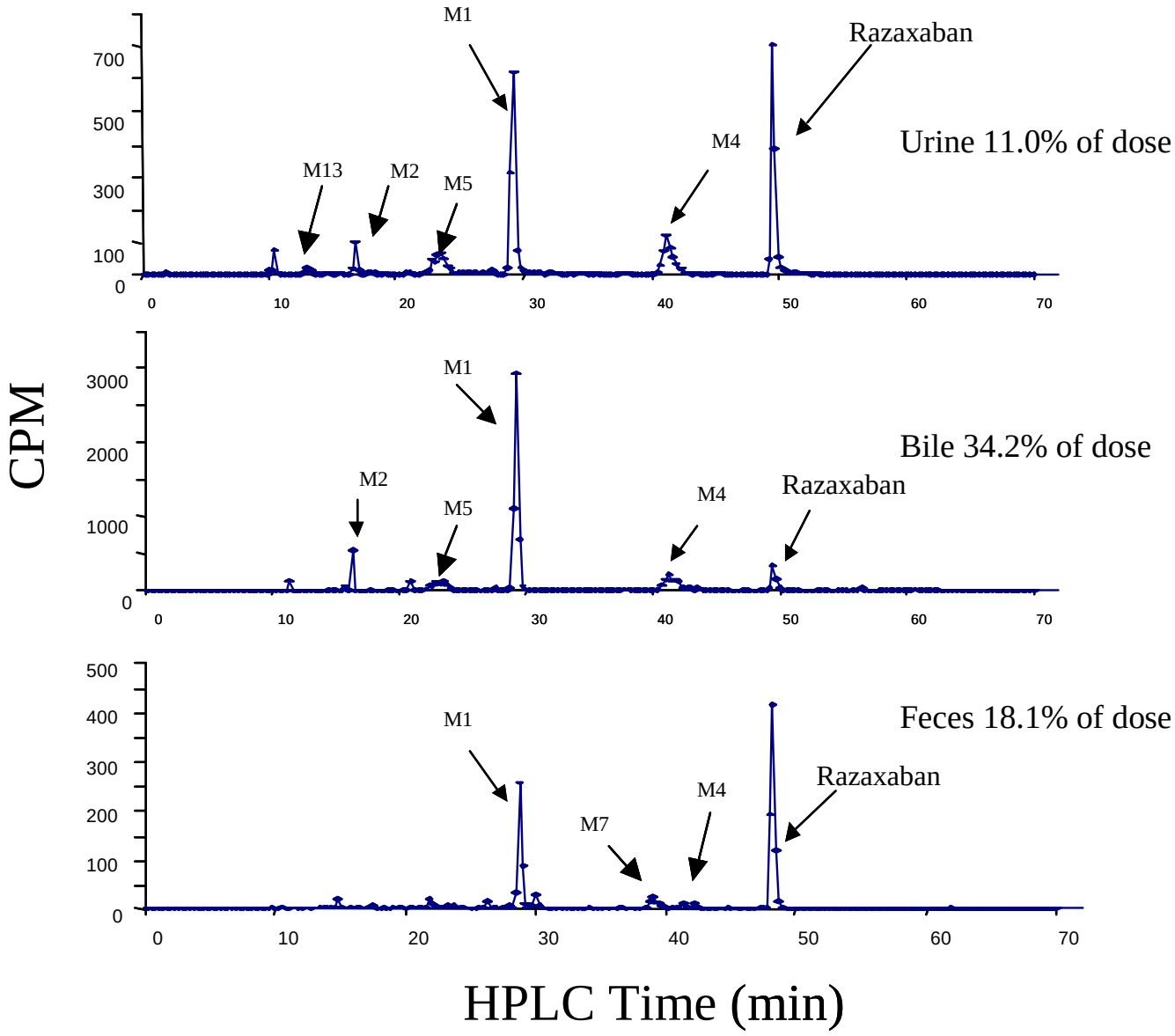

Downloaded from dmd.aspetjournals.org at ASPET Journals on April 17, 2024

DMD Fast Forward. Published on November 5, 2007 as DOI: 10.1124/dmd.107.018416
This article has not been copyedited and formatted. The final version may differ from this version.

Figure 6

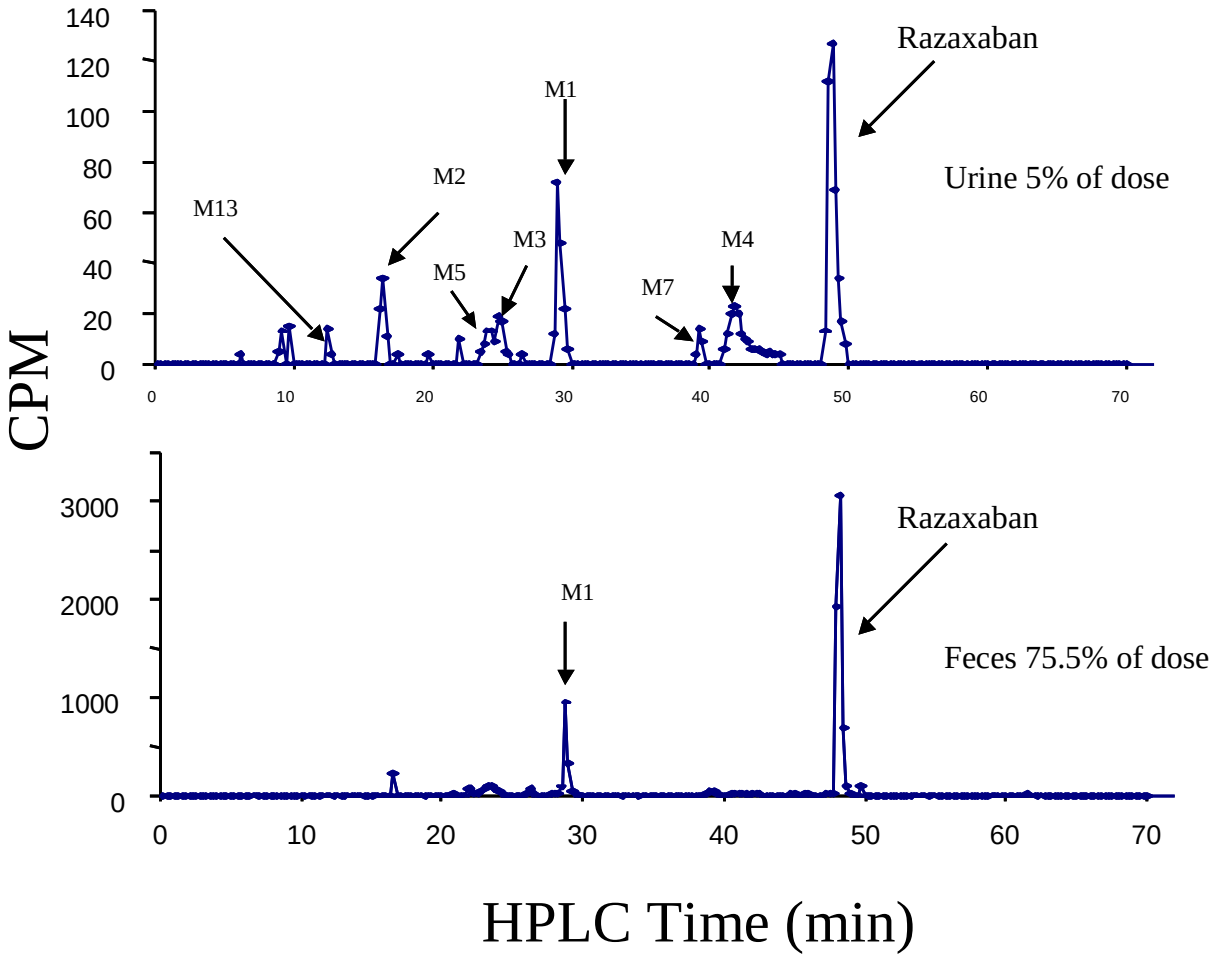

Downloaded from dmd.aspetjournals.org at ASPET Journals on April 17, 2024

DMD Fast Forward. Published on November 5, 2007 as DOI: 10.1124/dmd.107.018416
This article has not been copyedited and formatted. The final version may differ from this version.

Figure 7

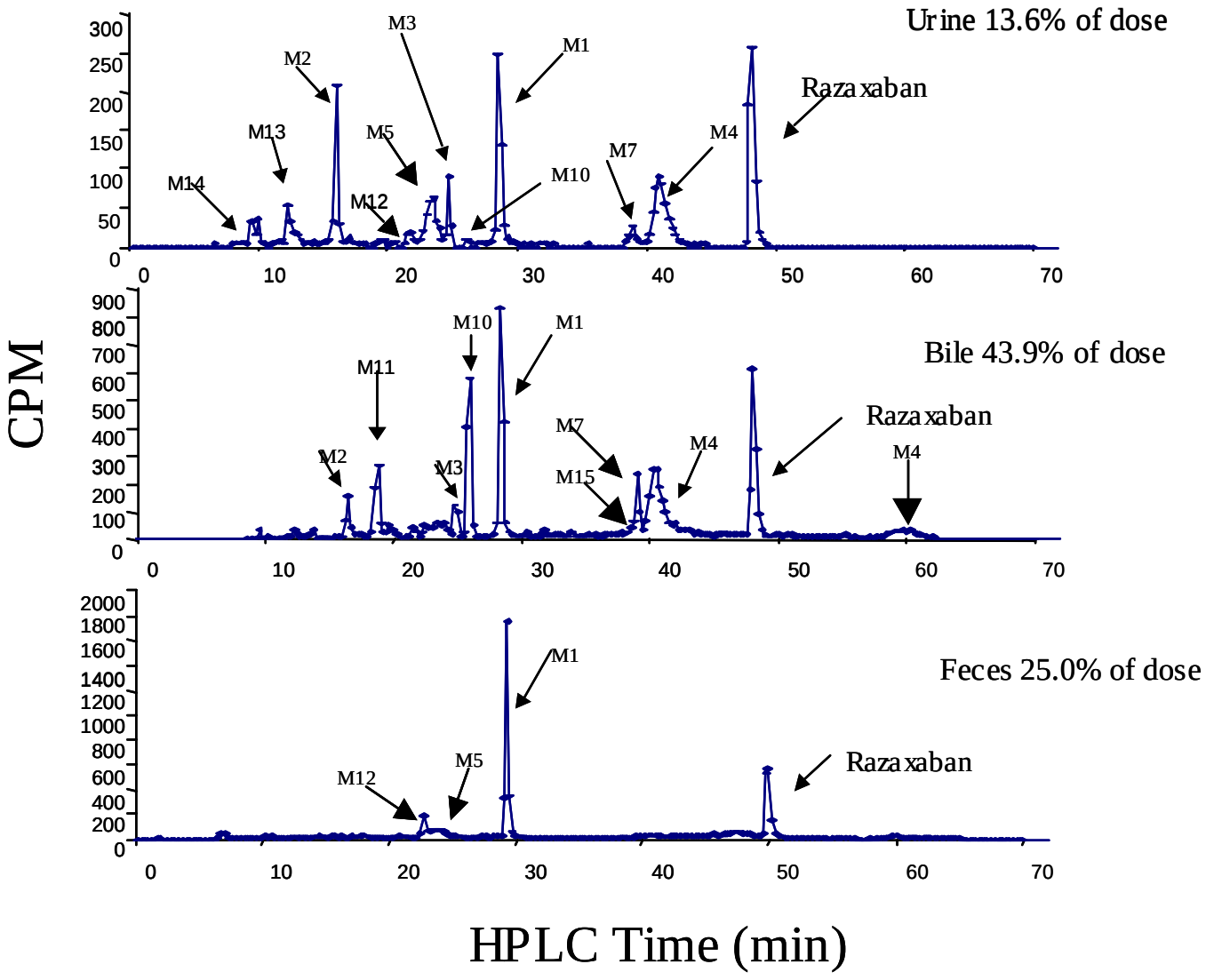

Downloaded from dmd.aspetjournals.org at ASPET Journals on April 17, 2024

DMD Fast Forward. Published on November 5, 2007 as DOI: 10.1124/dmd.107.018416
This article has not been copyedited and formatted. The final version may differ from this version.

Figure 8

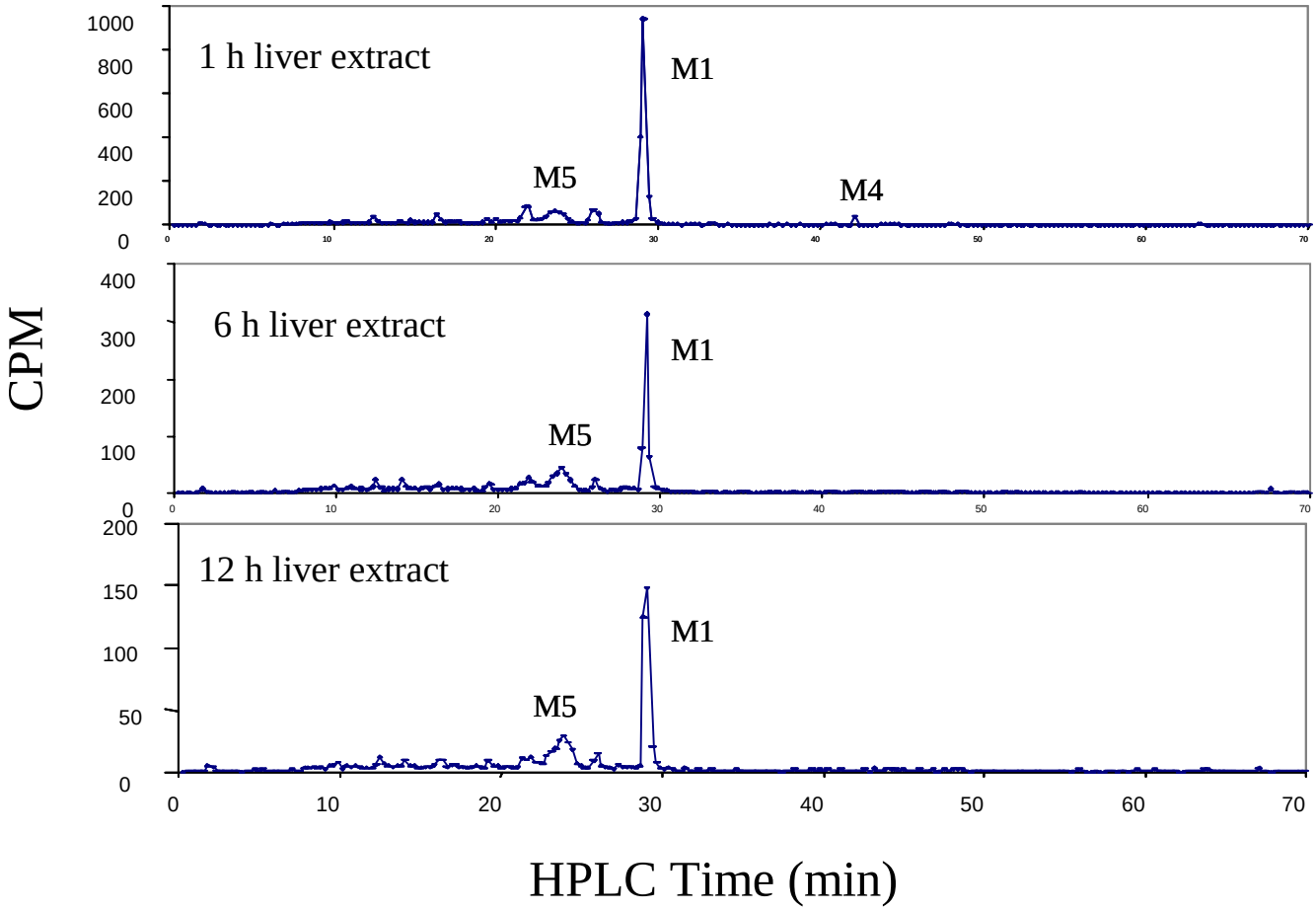

Downloaded from dmd.aspetjournals.org at ASPET Journals on April 17, 2024

DMD Fast Forward. Published on November 5, 2007 as DOI: 10.1124/dmd.107.018416
This article has not been copyedited and formatted. The final version may differ from this version.

Fig 9

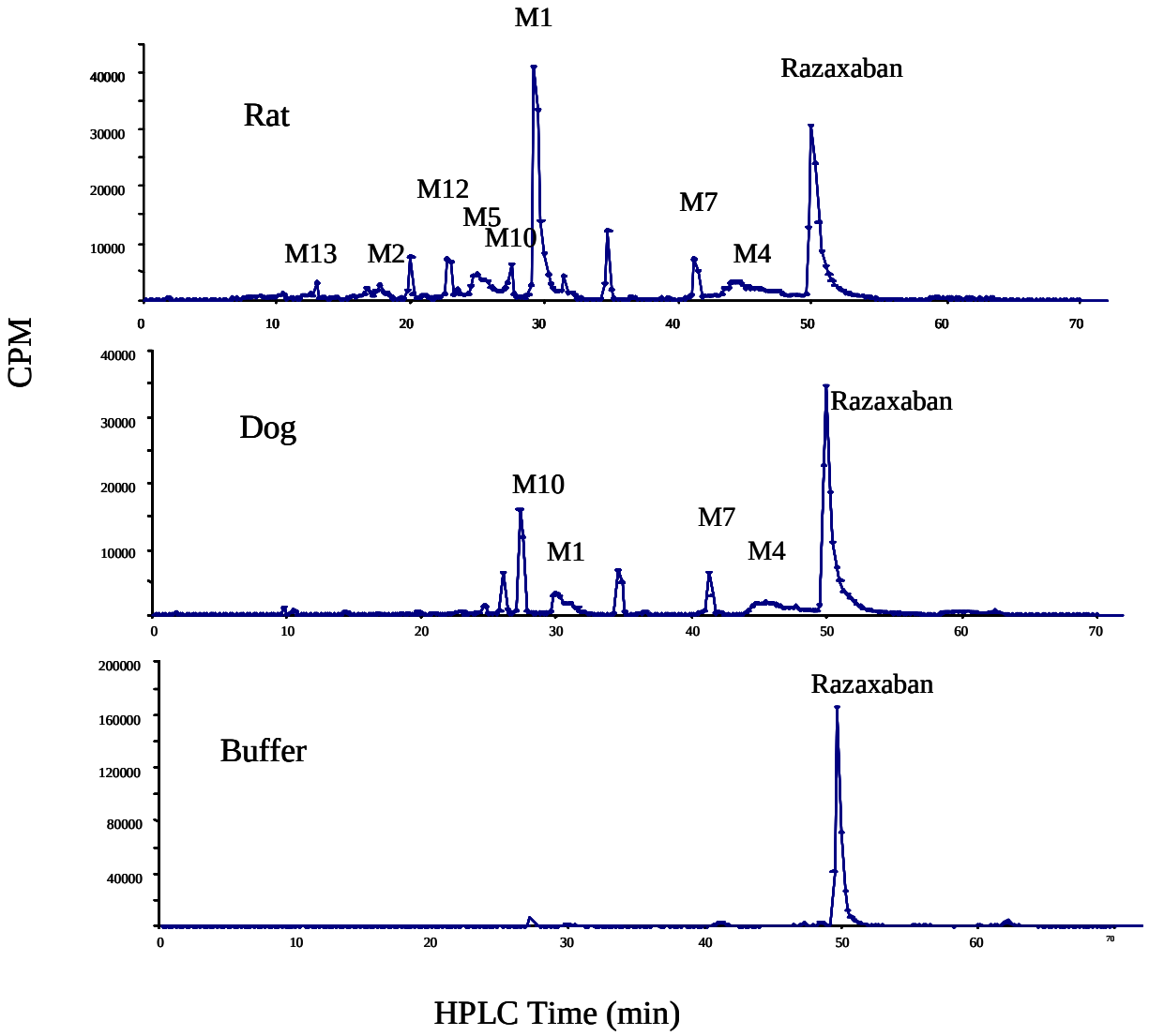

Downloaded from dmd.aspetjournals.org at ASPET Journals on April 17, 2024